การวิเคราะห์ฮาร์มอนิกเรโซแนนซ์ในระบบไฟฟ้ากำลังที่มีโรงไฟฟ้าพลังงานลม

นายชู ซวน ฮวน

วิทยานิพนธ์นี้เป็นส่วนหนึ่งของการศึกษาตามหลักสูตรปริญญาวิศวกรรมศาสตรมหาบัณฑิต
สาขาวิชาวิศวกรรมไฟฟ้า ภาควิชาวิศวกรรมไฟฟ้า
คณะวิศวกรรมศาสตร์ จุฬาลงกรณ์มหาวิทยาลัย
ปีการศึกษา 2556

HARMONIC RESONANCE ANALYSIS OF POWER SYSTEMS WITH A WIND POWER PLANT

Mr. Chu Xuan Huan

A Thesis Submitted in Partial Fulfillment of the Requirements
for the Degree of Master of Engineering Program in Electrical Engineering
Department of Electrical Engineering
Faculty of Engineering
Chulalongkorn University
Academic Year 2013

Thesis Title	HARMONIC RESONANCE ANALYSIS OF POWER SYSTEMS WITH A WIND POWER PLANT
By	Mr. Chu Xuan Huan
Field of Study	Electrical Engineering
Thesis Advisor	Assistant Professor Thavatchai Tayjasanant, Ph.D.

Accepted by the Faculty of Engineering, Chulalongkorn University in Partial Fulfillment of the Requirements for the Master's Degree

.....Dean of the Faculty of Engineering

(Professor Bundhit Eua-arporn, Ph.D.)

THESIS COMMITTEE

.....Chairman

(Channarong Banmongkol, Ph.D.)

.....Thesis Advisor

(Assistant Professor Thavatchai Tayjasanant, Ph.D.)

.....Examiner

(Surachai Chaitusaney, Ph.D.)

.....External Examiner

(Chakphed Madtharad, Ph.D.)

ชู ซวน ฮวน : การวิเคราะห์ฮาร์มอนิกเรโซแนนซ์ในระบบไฟฟ้ากำลังที่มีโรงไฟฟ้าพลังงานลม. (HARMONIC RESONANCE ANALYSIS OF POWER SYSTEMS WITH A WIND POWER PLANT) อ.ที่ปรึกษาวิทยานิพนธ์หลัก: ผศ. ดร.ธวัชชัย เตชัสอนันต์, 87 หน้า.

ปรากฏการณ์ฮาร์มอนิกเรโซแนนซ์เป็นปัญหาสำคัญที่ส่งกระทบต่อผู้ผลิตไฟฟ้าและวิศวกรเป็นเวลานานหลายปี ปัจจุบันพลังงานลมจัดเป็นแหล่งพลังงานหมุนเวียนที่ได้รับความนิยมเป็นอย่างมาก เนื่องจากเป็นพลังงานสะอาดและยั่งยืน ดังนั้นการนำโรงไฟฟ้าพลังงานลมเข้าสู่โครงข่ายไฟฟ้าถือเป็นความท้าทายในการศึกษาปรากฏการณ์ฮาร์มอนิกเรโซแนนซ์ วิทยานิพนธ์นี้มีวัตถุประสงค์เพื่อพิจารณาการเกิดฮาร์มอนิกเรโซแนนซ์และเส้นทางการเกิดเรโซแนนซ์ในระบบไฟฟ้าที่มีการเชื่อมต่อกับโรงไฟฟ้าพลังงานลมด้วยการแก้ปัญหาตามวิธีดีเทอมินิสติก โดยวิธีนี้เป็นการเปรียบเทียบข้อดีและข้อเสียของการวิเคราะห์ภายใต้โดเมนความถี่ซึ่งประกอบด้วยวิธีการวิเคราะห์โดยการสแกนความถี่ และวิธีการวิเคราะห์โหมดของฮาร์มอนิกเรโซแนนซ์ สำหรับวิธีในวิทยานิพนธ์ฉบับนี้เลือกใช้วิธีการวิเคราะห์โหมดของฮาร์มอนิกเรโซแนนซ์ เนื่องจากวิธีดังกล่าวสามารถให้ข้อมูลที่มีประโยชน์ในการวิเคราะห์ทางฮาร์มอนิกได้ และวิธีนี้ถูกนำไปใช้ในระบบไฟฟ้าที่มีการเชื่อมต่อกับโรงไฟฟ้าพลังงานลมที่มีแบบจำลองเป็นไปตามศูนย์ปฏิบัติการพลังงานทดแทนแห่งชาติ (National Renewable Energy Laboratory - NREL) ของประเทศสหรัฐอเมริกา ผลลัพธ์ที่ได้จากการจำลองได้มีการตรวจสอบผลที่ได้จากข้อมูลการวัดที่เกิดขึ้นจริงซึ่งเป็นการเก็บรวบรวมจากฟาร์มกังหันลมแห่งแรกในประเทศไทยและจากการตรวจสอบผลลัพธ์ที่ได้พบว่าวิธีการวิเคราะห์ฮาร์มอนิกเรโซแนนซ์สามารถใช้ในการวิเคราะห์ฮาร์มอนิกเรโซแนนซ์ นอกจากนี้ในการตรวจสอบพบว่าการศึกษาฮาร์มอนิกรองรับแบบจำลองที่เสนอโดย NREL อีกด้วย

ภาควิชา วิศวกรรมไฟฟ้า ลายมือชื่อนิสิต .....

สาขาวิชา วิศวกรรมไฟฟ้า ลายมือชื่อ อ.ที่ปรึกษาวิทยานิพนธ์หลัก .....

ปีการศึกษา 2556

5470571221 : MAJOR ELECTRICAL ENGINEERING
KEYWORDS: HARMONIC RESONANCE ANALYSIS / MODAL ANALYSIS / WIND POWER PLANT / EQUIVALENT MODEL / HARMONIC DISTORTION

CHU XUAN HUAN: HARMONIC RESONANCE ANALYSIS OF POWER SYSTEMS WITH A WIND POWER PLANT. ADVISOR: ASST. PROF. THAVATCHAI TAYJASANANT, Ph.D., 87 pp.

Harmonic resonance phenomenon is a problem paid attention significantly from utilities and electrical engineers for many years. Nowadays, wind power is the leading renewable source, which is considered as the solution for a clean and sustainable resource; however, the integration of wind power plants into grids brings challenges for harmonic resonance study. The objective of this thesis consists of two issues that are determining potential harmonic resonances and resonance paths in power systems connected with a wind power plant. The solution based on deterministic methods has pointed out by comparing pros and cons among available methods in frequency domain including frequency scan analysis, harmonic resonance mode analysis and state-space based method. The thesis selected harmonic resonance mode analysis in the light of the useful information provided by this method. The method is conducted in a practical power systems connected with a wind power plant when the wind power plant is modeled as an equivalent model based on the method that is proposed by National Renewable Energy Laboratory (NREL), which is one of important laboratories of the United States. The simulation results are then verified with field measurement data collected from the first wind farm in Thailand. The verification figures out that the results found by using harmonic resonance mode analysis is valid in harmonic resonance analysis. Moreover, the verification also supports that the equivalent model proposed by NREL is applicable in harmonic studies.

Department: Electrical Engineering Student's Signature .....
Field of Study: Electrical Engineering Advisor's Signature .....
Academic Year: 2013

ACKNOWLEDGEMENTS

This work has been conducted at Power System Research Laboratory (PSRL), Department of Electrical Engineering, Chulalongkorn University. The financial support by ASEAN University Network/ Southeast Asia Engineering Education Development Network (AUN/SEED – Net) Program of Japan International Cooperation Agency (JICA) is gratefully appreciated.

First of all, I would like to take this opportunity to express my deepest gratitude to my thesis supervisor, Assistant Professor Thavatchai Tayjasanant, for his advice, patient guidance, and caring throughout my study at Chulalongkorn University. Those inspirational talks with him have truly motivated me to go through the long term of doing research. Without his enthusiastic encouragement and support, the thesis would never have been completed.

I also would like to extend my thanks to Dr. Chakphed Madtharad for his kind help during field measurement data collection.

My sincere thanks go to the committee members including Dr. Channarong Banmongkol, Dr. Surachai Chaitusaney, and Dr. Chakphed Madtharad for their valuable time and technical suggestion to fulfil my work. I would like to thank to all professors, lecturers at Chulalongkorn University, who provided me great lectures that help me get an overview picture of power system engineering. I also would like to extend my thanks to all members at Power System Research Laboratory (PSRL) for their encouragement and kind help during my study in Thailand. My appreciation also goes to Dr. Ghassemi, Dr. Kah-Leong Koo, Dr. Cui for those explanations of their works.

Finally, I wish to thank my parents, my beloved sister for their support and unconditional love throughout my study.

CONTENTS

Page

Page

Page

LIST OF FIGURES

LIST OF TABLES

CHAPTER I

Introduction

1.1 Introduction

Nowadays, a large amount of power electronic-based devices is connected to electric power systems. These devices behave like nonlinear devices and generate harmonics into grids. Moreover, the use of renewable energy sources such as wind power is increasing due to a demand of clean energy when the possibility of scarcity of fossil energy resources and pollution problem from the power plants that are running on these resources is forthcoming. Wind power is exploited increasingly in energy policy of each country over the world. However, the integration of wind power plants into the power system supported by power electronic interfaces possibly results in harmonic relating issues such as harmonic distortion, harmonic resonances and so on. These problems can affect negatively to power quality, particularly voltage and current quality.

1.2 Motivation

Harmonic resonances should be an issue paid attention when considering power systems connected to wind power plants. Although wind power plants generate inappreciable harmonics into grids, possibility of harmonic resonances is unavoidable. Assessing harmonic propagation and analyzing origins of harmonics causing harmonic resonances are crucial. Operating condition of wind power plants is distinct to the conventional power plants due to impacts of variable wind speed and geographic location. As a result, harmonic resonance analysis in grids connected wind power plants is also more challengeable than that in traditional grids. The reliable information from harmonic resonance analysis will help utilities and system engineers prevent power systems from risky problems. Furthermore, the integration compliance issue will be taken into account better in the light of the additional information provided from harmonic resonance study.

So far, frequency scan analysis is still the prominent method used for identifying harmonic resonance frequencies. However, a little information provided by this method leads to require an improvement or other methods that can bring more information about possible resonances. Recently, harmonic resonance mode analysis proposed has been paid attention significantly in harmonic study. This method has overcome restrictions of frequency scan analysis; the information provided is not only resonance frequencies but also includes the buses participating during harmonic

resonances and so on. Besides harmonic resonance mode analysis, state-space based method, which also is developed on modal analysis, has presented well in harmonic resonance study. Nonetheless, when analyzing each method's advantages and disadvantages, harmonic resonances mode analysis (HRMA) shows more advantageous. Thus, conducting this method in harmonic resonance analysis in grids connected wind power plants is a valuable task in order to achieve the goal of detecting and attenuating possible resonances effectively.

1.3 Objectives

The work in this thesis is to analyze harmonic resonances in power systems when a wind power plant is integrated into systems. There are two objectives presented in this thesis:

1. To analyze harmonic resonances in power systems with a wind power plant
2. To determine the resonance path during resonances

1.4 Scope of Study

1. The research focuses mainly on harmonic resonance analysis.
2. Parallel is the main interest in this thesis due to its frequent occurrence and more serious impact than series resonance.
3. Electric power systems are assumed to be balanced system.
4. Harmonic resonances are analyzed in the study up to 2500 Hz referring to 50 Hz fundamental frequency of system.
5. Variable speed wind generator types III and IV are considered mainly in harmonic resonance analysis.

1.5 Methodology

1. Perform literature reviews on background knowledge about harmonic resonance analysis and equivalent models of wind power plants.
2. Collect necessary data
3. Conduct harmonic resonance mode analysis and modal sensitivity indices
4. Develop a program that is capable of harmonic resonance analysis based on harmonic resonance mode analysis
5. Analyze the phenomenon based on theoretical and actual data
6. Verify results and improve the developed program

The methodology is summarized in Figure. 1.1.

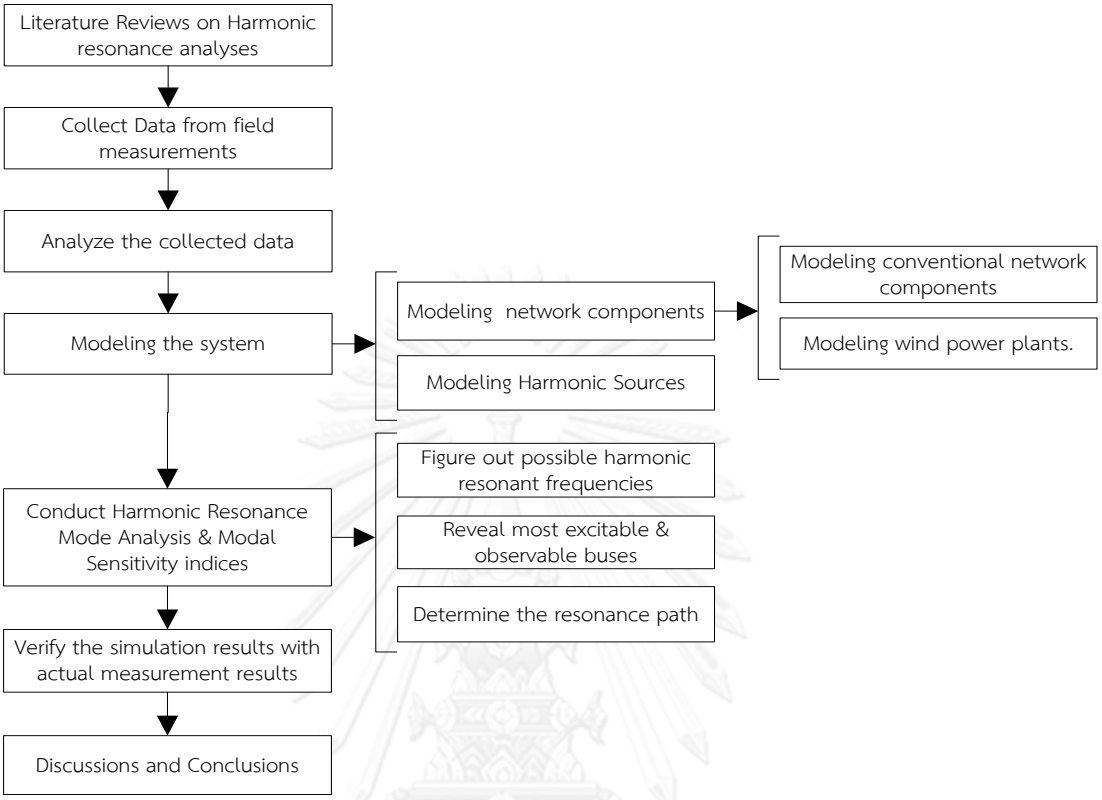

Figure 1.1 The methodology

1.6 Expected Contribution

The information provided from harmonic resonance analysis is useful to construct the resonance paths. These resonance paths constructed will help utilities and system engineers in design stage of power systems when an integration of wind power plants is taken into account. Moreover, conducting harmonic resonance analysis also helps figure out the most network components and main aspects influencing on harmonic resonances. This information is necessary not only for planning in case of system expansion, but also for preventing systems from negative effects of resonances.

1.7 Outline of Thesis

The thesis contains six chapters presented as follows.

Chapter 2 presents general understanding about harmonic resonances in term of definition and their impacts on power systems. Harmonic resonances are considered in power systems with a wind power plant; therefore, general configuration of wind

turbine generators is summarized in order to help point out harmonic components that are possible to cause harmonic resonances. This chapter also presents some standards used for assessing harmonic resonances in power system.

Chapter 3 summarizes literature reviews of available methods for harmonic resonance analysis and harmonic models of wind power plants. Those noticeable methods for harmonic resonance analysis are summarized in this chapter. Based on this summary, a comparison is also presented in order to figure out the suitable method for harmonic resonances.

Chapter 4 presents problem formulation, and a methodology is conducted for analyzing harmonic resonances. A verification procedure is also presented in this chapter. The verification with field measurement data is used in order to validate the simulation results.

Chapter 5 shows simulation results and verification with actual measurement data. The discussion is presented in this chapter as well.

Chapter 6 concludes the study, and future work is also suggested.

CHAPTER II

Harmonic Resonances in Power Systems with Wind Power Plants

The chapter aims to provide an overview of harmonic resonances in power systems. Definition in accordance with current international standards including the Institute of Electrical and Electronic Engineer (IEEE) and International Electro-technical Commission (IEC), and categories of harmonic resonances are presented. Furthermore, this chapter also elaborates harmonic issues in wind power plants by summarizing the state of the art of electronic applications for wind turbines. Based on these summaries, this chapter provides useful information and explains possibility of potential harmonic resonances in power systems with wind power plants.

2.1 Harmonic Resonances

The IEEE and IEC standards are widespread standards used throughout the world. Therefore, both standards are considered as main standards in this study. The fundamental perception of harmonics is regarded to both standards.

2.1.1 Resonance Definition

Harmonic resonances are mentioned in both IEEE 519-1992 and IEC 61000-3-6 standards [1, 2]. Generally, harmonic resonance can be defined as a phenomenon that happens in power systems when a natural frequency produced by power systems containing both inductive and reactive components coincides with a frequency generated from harmonic sources incorporated into those power systems [3].

2.1.2 Harmonic Resonance Categories

The classification of harmonic resonance types depends on the direction of harmonic current flows that result in resonances in power systems. Harmonic resonances can be categorized into two types: series and parallel resonances [1, 2]. Although most of serious problems of resonances are parallel resonance, it is more general to present both types of resonances in this part. Figure. 2.1 depicts potential harmonic resonances.

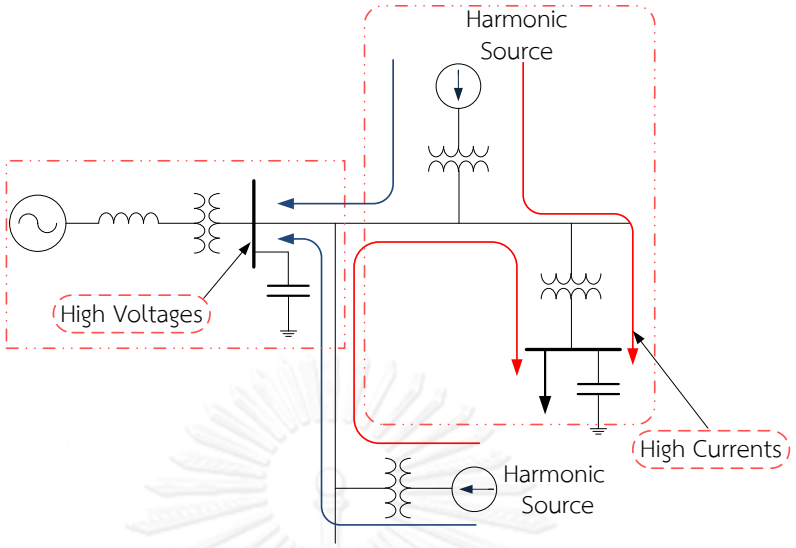

Figure 2.1 The system with potential parallel and series resonances [3]

2.1.2.1 Parallel Resonance

Regarding IEEE 519 standard [1], parallel resonance happens in power systems is described as follows.

The harmonic current flows into the system through reactive and inductive elements that are parallel connected to each other in accordance with the direction of harmonic current flow. At a certain frequency of harmonic sources, the reactance and inductance of those aforementioned elements are cancelled each other, which lead to the largest impedance seen from bus injected by the harmonic current. This largest impedance results in very high voltage at the bus of interest, and harmonic currents flowing through those reactive and inductive elements are magnified as well. This phenomenon is called parallel resonance. The direction of harmonic current resulting in parallel resonance can be depicted in Figure. 2.2.

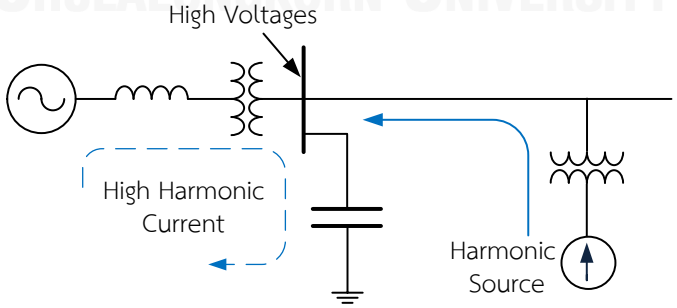

Figure 2.2 Potential parallel resonance

2.1.2.2 Series Resonance

Series resonance results from cancellation of reactive and inductive impedance of the corresponding elements at a certain harmonic frequency. These inductive and reactive elements are connected in series in accordance with the flow of harmonic currents through power systems. Series resonance leads to very low impedance seen from bus injected by harmonic sources, which can cause considerably high voltage distortion and harmonic currents.

Figure. 2.3 describes the direction of harmonic current that can account for series resonance.

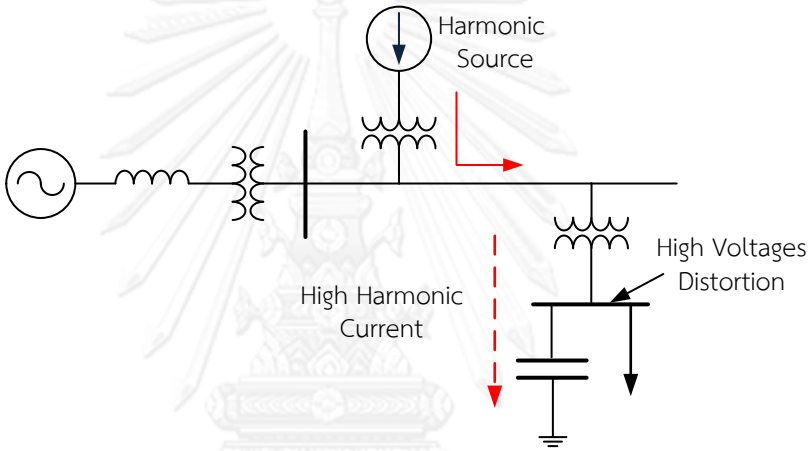

Figure 2.3 Potential series resonance

2.1.3 Impacts of Harmonic Resonances on Power Systems

The influences of harmonic resonances on power systems are documented rather well in IEEE 519-1992 and IEC 6100-3-6 standards [1, 2]. The main impacts of harmonic resonances on power system can be summarized in following points:

- Fundamentally, harmonics resonances persist harmonic currents and voltages at very high values. Those harmonic currents and voltages result in very high harmonic distortion, which leads to maloperation of power apparatus in grids.

- High values of harmonic voltages and currents due to harmonic resonances also cause unsuccessful integration of distributed generation into power systems such as wind power plants and photovoltaic.

- Harmonic resonances take place frequently in power systems incorporating capacitor banks, which can account for serious failure of capacitor banks due to over currents and over voltages in such resonances [3].

2.2 Harmonic Resonance Issues in Wind Power Plants

Wind power plants are playing a role of harmonic sources in electric power systems. The electronic applications used account for generation of harmonics into main grids. The perception of power electronic applications for wind turbines is necessary to harmonic resonance study.

2.2.1 Power Electronic Applications for Wind Turbines

Wind turbines can be classified into two main categories: fixed speed and variable speed turbines. Furthermore, wind turbines can also be categorized as four major types known as type I, II, III and IV. Type I refers to fixed speed wind turbines. Type II refers to limited variable speed wind turbines and type III and IV refer to variable speed wind turbines [4-7]. The wind turbine generators used include both synchronous and induction generators.

The configuration of wind turbines connected with grids is shown in Figure 2.4.

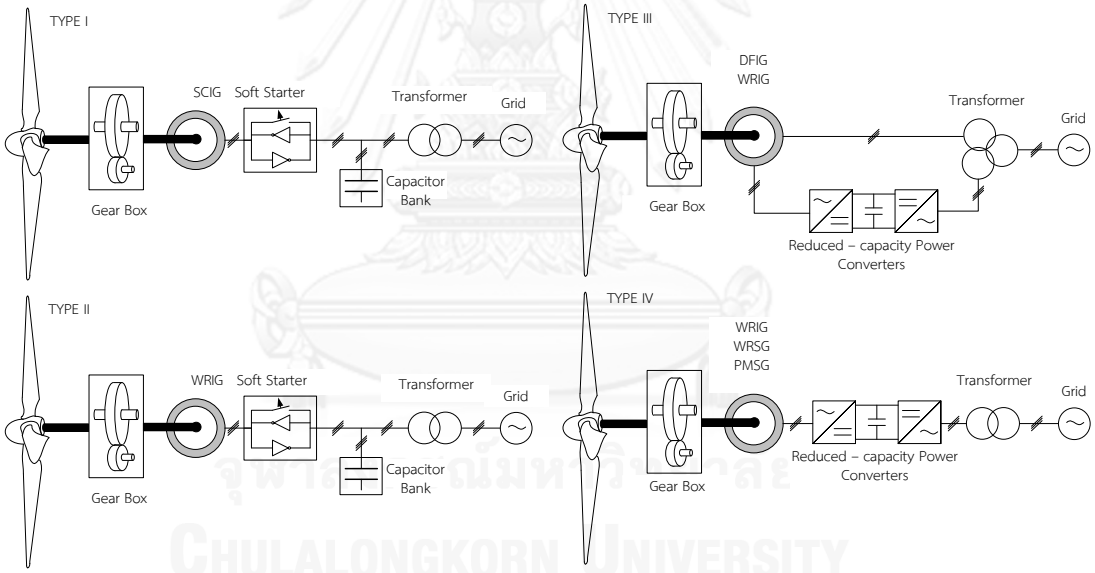

SCIG : Squirrel Cage Induction Generator

WRIG: Wound Rotor Induction Generator

WRSG: Wound Rotor Synchronous Generator

PMSG : Permanent Magnet Synchronous Generator

Figure 2.4 Wind turbine configurations [6, 7]

A further classification of wind turbines is based on the type of power control: stall, pitch, and active stall. This classification is described in Table 2.1.

Table 2.1 Wind turbine categories classified by power control [7]

Speed Control		Power control		
		Stall	Pitch	Active stall
Fixed speed	Type I	Type I0	Type I1	Type I2
Variable speed	Type II	*Type II0	Type II1	*Type II2
	Type III	*Type III0	Type III1	*Type III2
	Type IV	*Type IV0	Type IV1	*Type IV2

* Note: those types with a star indicate that there is no combination between speed and power control topologies [7].

Fixed speed and variable speed wind turbines configured by popular power electronic applications are presented more in details in next sections [5], [7], [8].

2.2.1.1 Soft Starter for Fixed Speed Wind Turbine Generators

The basic configuration of a fixed speed wind turbine is shown in Figure. 2.4 type I. The squirrel cage induction generator (SCIG) is connected to the step – up transformer through a soft starter. The soft starter is configured by six thyristors, which are equipped in two per phase in anti-parallel. The connection of wind turbine generators to system results in high inrush currents that trigger disturbances in systems. RMS value of inrush currents is limited due to application of soft starter [5].

2.2.1.2 Power Electronics for Variable Speed Wind Turbines

Nowadays, the technology for speed control in wind turbines has shifted from fixed speed to variable speed wind turbines, which aims to fulfill the requirement of maximizing captured power and reducing mechanical stress. The most popular configuration of variable speed wind turbines is known as doubly fed induction generator (DFIG) and full rated converter wind turbines [8].

- Doubly Fed Induction Generator (DFIG) Wind Turbines

The configuration of DFIG wind turbine is depicted as type III in Figure. 2.4. A back-to-back converter is used to supply the current from the grid to the rotor of the generator. Figure 2.5 depicts a system configuration of a DFIG, which is the same as the configuration in Figure 2.4.

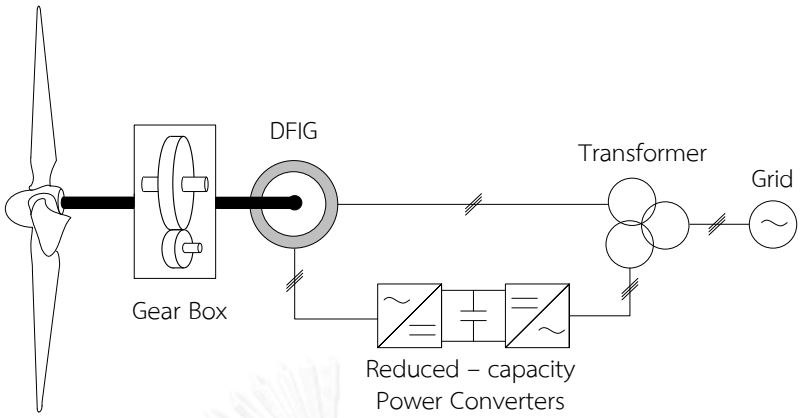

Figure 2.5 The system configuration of a DFIG [6]

The converter consists of two bidirectional converters connected together by a common DC link. The converter used in this configuration is capable of controlling both the active and reactive power supplied to electric power systems.

- Full Rated Converter (FRC) Wind Turbines

The most common configuration of a full rated converter (FRC) wind turbine is depicted as type IV in Figure. 2.4. Generators can be one of three types of generators, which are permanent magnet multi-pole synchronous generator (PMSG), wound rotor induction generator (WRIG), and wound rotor synchronous generator (WRSG). A back-to-back converter is usually used to connect wind turbine generators to grids. The configuration of the converter is similar to the converter used in DFIG wind turbine.

2.2.2 Harmonic Emission

Generally, harmonic emission from those wind turbine generators without electronic converters including fixed speed wind turbine generators type I and limited speed wind turbines type II is not known of serious problems with grids or customers [6], [7]. Nonetheless, for those variable speed wind turbines, harmonic emission needs to be paid attention. Inverters and converters in wind turbines with DFIG or FRC are origins of harmonics in power system [6], [7]. The contents of harmonics depend considerably on the switching frequency used in equipped converters. Pulse width modulated (PWM) inverters designed with the switching frequencies in the range of 2 – 3 kHz can produce harmonics in the range of some kilohertz [7]. Figure. 2.6 depicts a spectrum of harmonic currents generated by a full rated converter wind turbine.

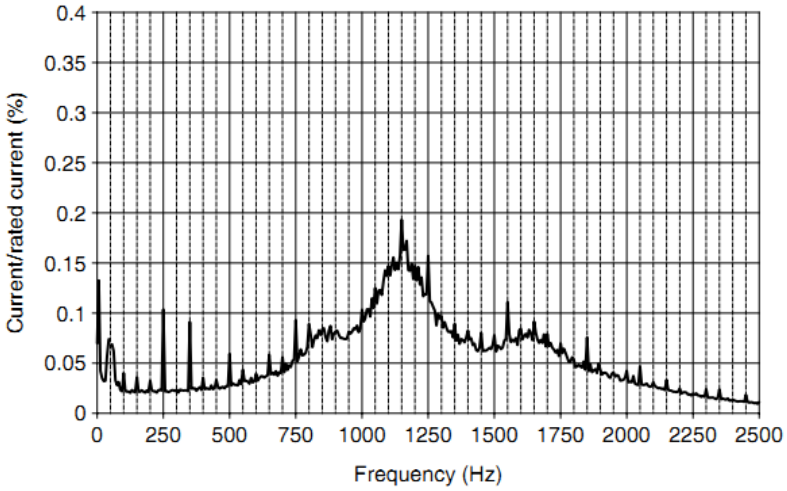

Figure 2.6 Harmonic current emission of a variable speed wind turbine [7]

2.3 Assessment of Harmonic Resonances

For assessing harmonic resonance in power systems connected with wind power plants, the IEC 61400-21 standard is considered as the main standard in the study [9]. The standard does not document specifically the compliance issues with harmonic resonances; however, impacts of harmonic resonances on voltages and currents are reasons to regard resonances with harmonic issues stated in IEC 61400-21 standard. IEC 61400-21 standard documents the applicable limits for harmonic emission that are referred to IEC 61000-3-6 standard [2, 9]. Regarding harmonic resonances, the indices characterizing harmonic resonances are total harmonic distortion (THD), which is calculated in term of voltage as

$$THD = \frac{\sqrt{\sum_{i=2}^{50} V_i^2}}{V_1} \tag{2.1}$$

where V1 is the voltage at fundamental frequency, and harmonic components are taken into account up to the 50^{th} .

Based on IEC 61000-3-6 standard, the total harmonic current at the point of common coupling is calculated as

$$I_{hs} = \sqrt[\beta]{\sum_{i=1}^{N_r} \left(\frac{I_{h,i}}{n_i} \right)^{\beta}} \tag{2.2}$$

where:

N_f : the number of wind turbine generators

I_h : the magnitude of the h-th harmonic generated by the i-th source.

n_i : the ratio of the transformer at the i-th wind turbine

β : the summation exponent is looked up in Table 2.2 below.

Table 2.2 Summation Exponents

Harmonic order	β
h < 5	1.0
$5 \leq h \leq 10$	1.4
h >10	2.0

The compliance limit for harmonics is addressed in IEC 61000-3-6 standard as in Table 2.3 [2].

Table 2.3 Voltage distortion limits for harmonics in low and medium voltage power systems

Odd harmonic non multiple of 3		Odd harmonics multiple of 3		Even harmonics	
Order h	Harmonic voltage %	Order h	Harmonic Voltage %	Order h	Harmonic Voltage %
5	6	3	5	2	2
7	5	9	1.5	4	1
11	3.5	15	0.3	6	0.5
13	3	21	0.2	8	0.5
17	2	> 21	0.2	10	0.5
19	1.5			12	0.2
23	1.5			> 12	0.2
25	1.5				
> 25	$0.2 + 1.3 \times \frac{25}{h}$				
NOTE – Total harmonic distortion (THD): 8%					

CHAPTER III

Harmonic Resonance Analyses and Modeling Wind Power Plants

Harmonic resonance analysis methods are summarized in this chapter. Based on this summary, the most suitable method is chosen for harmonic resonance study. In addition, this chapter presents the model of wind power plants used in the research.

3.1 Reviews on Harmonic Resonance Analyses

Harmonic resonance phenomenon happens in a power system when the system frequency coincides with one of the frequencies generated from harmonic sources. Harmonic resonances result in high increase of voltages and currents flowing through the system. The methods used for harmonic resonance analysis can be classified into two main classes, the former class of the method is known as frequency scan analysis, and the latter ones are the methods based on modal analysis [10]. The noticeable differences among these methods including theoretical understanding and implementation issues have been documented well in [10]. Methods based on modal analysis include mainly harmonic resonance mode analysis and state-space model based analysis [11-15]. Basically, the methods for analyzing harmonic resonances can be classified as shown in Figure. 3.1.

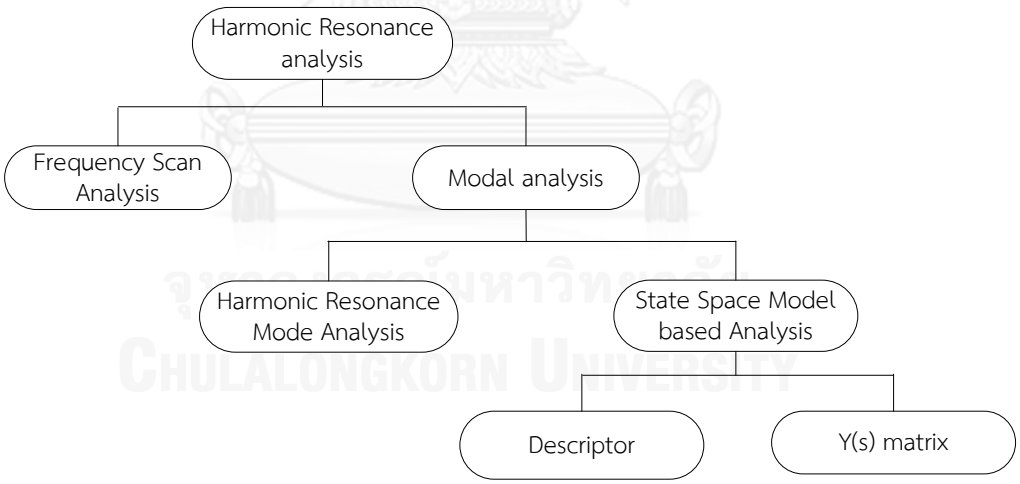

Figure 3.1 Classification of harmonic resonance analysis method

3.1.1 Frequency Scan Analysis

The most common method for harmonic resonance analysis is known as frequency scan analysis [16, 17]. Frequency scan analysis is based on characteristics of harmonic impedance matrix to construct the system response as a function of frequency. The method can be summarized briefly as follows.

$$[I]_h = [Y_{bus}]_h [V]_h \quad (3.1)$$

$$[V]_h = [Y_{bus}]_h^{-1} [I]_h = [Z_{bus}]_h [I]_h \quad (3.2)$$

where:

h : harmonic order

$[Y_{bus}]_h$: system admittance matrix

$[Z_{bus}]_h$: system impedance matrix

$[I]_h$: harmonic current injection

$[V]_h$: bus voltage matrix

Since Y_{bus} and Z_{bus} contain linear elements; this linear property can be used for estimating bus voltages as in the equation (3.2). The voltage of a bus of interest are calculated by using a harmonic current source with the value of $1\angle 0^{\circ}$ (A or p.u) that injected directly into this bus while other harmonic sources at remaining buses are grounded. By doing in similar manner for various harmonic frequencies, voltages of the buses of interest at different frequencies are determined. The curve plotted by voltages against corresponding harmonic frequencies is known as frequency scan curve. This curve shows the resonance points that are indicated by the peaks (the highest impedance associated with parallel resonance) and the valleys (the lowest impedance associated with series resonance) as illustrated in Figure. 3.2.

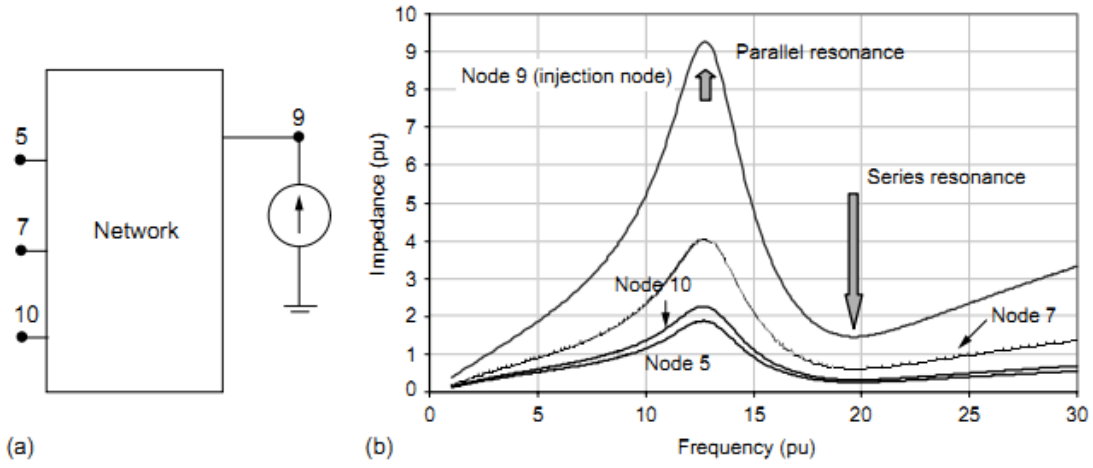

(a) Simulated system (b) Frequency response in frequency domain

Figure 3.2 Frequency response of a system with resonances [17]

The frequency scan analysis is a simple method that allows identifying the resonance frequency easily, but this method does not show the components affecting directly harmonic resonance, and lacks of additional information to solve harmonic

resonance effectively as well. Moreover, this method is time consuming because it needs to the invert an admittance matrix.

3.1.2 Harmonic Resonance Mode Analysis

The later method developed by using the modal theory is harmonic resonance mode analysis (HRMA) [15, 17]. As compared in the [10], the proposed method has overcome the restriction of previous methods. Furthermore, that harmonic resonance mode analysis allows presenting the responses in the frequency domain, and bringing a familiar approach in harmonic resonance assessment. HRMA not only figures out correctly the harmonic resonance points but also reveals observable and excitable buses in power system. The results found by harmonic resonance mode analysis are considerably informative. The following studies in [10, 18-22] continue advancing and representing the validity of the proposed method. Harmonic resonance mode analysis can solve well both resonance phenomena. Although the method shows some drawbacks as there are two different approaches in analyzing series and parallel resonance, the information provided by HRMA is worth taking into account in harmonic resonance analysis.

The method is based on the eigen - decomposition by considering the singularity characteristic of system admittance matrix. These characteristics are worthwhile to harmonic resonance study when each eigenvalue is close to zero or considerably small resulting in very high voltage. Harmonic resonance analysis can be understood from

$$[V]_f = [Y]_f^{-1}[I]_f \tag{3.3}$$

where $[Y]_f$ is the system admittance matrix at harmonic frequency f, and $[V]_f$ and $[I]_f$ are the node voltage and nodal current injection respectively. Assuming that harmonic resonance happens at the frequency f in the system, the subscript f will be omitted hereinafter for convenience. The matrix $[Y]$ can be decomposed in accordance with the matrix theory [23].

$$[Y] = [L][\Lambda][T] \tag{3.4}$$

where:

L (= $[l_1, l_2,...,l_n]$) and T (= $[t_1, t_2,..., t_n]$)^T : the left and right eigenvector respectively $[L] = [T]^{-1}$. Super script T demonstrates matrix transpose.

$[\Lambda]$: the diagonal admittance matrix with eigenvalues $\lambda_1,...,\lambda_n$

$$[\Lambda]=\begin{bmatrix} \lambda_1 & 0 & \dots & 0 \\ 0 & \lambda_2 & . & 0 \\ 0 & . & \dots & 0 \\ 0 & 0 & \dots & \lambda_n \end{bmatrix} \tag{3.5}$$

The modal impedance matrix is obtained by the inverse of $[\Lambda]$ as follows.

$$[V]=[L][\Lambda]^{-1}[T][I] \tag{3.6}$$

$$[T][V]=[\Lambda]^{-1}[T][I] \tag{3.7}$$

By defining $[U] = [T][V]$ or $[V] = [T]^{-1}[U] = [L][U]$ and $[J] = [T][I]$, the equation (3.7) is written as

$$[U]=[\Lambda]^{-1}[J] \tag{3.8}$$

From the equation (3.6) (3.7) and (3.8), inverse of eigenvalue is called modal impedance. The smallest eigenvalue is named a critical eigenvalue. Since [*L*] and [*T*] are constant matrices, those vectors [*U*] and [*J*] are proportional to [*V*] and [*I*] respectively. The frequency corresponding to the critical eigenvalue is called the critical mode frequency. The plot of modal impedance as a function of the frequency can reveal the point of resonance. The corresponding left and right eigenvectors will characterize the locations that are observable and excitable buses of critical mode respectively.

Moreover, the method offers modal sensitivity indices, which are modal impedance [10] and modal frequency sensitivities [22]. These indices are taken into account importantly in harmonic mitigation scheme [22], which can be calculated as follows.

Modal impedance sensitivity

$$\left.\frac{\partial\lambda}{\partial\alpha}\right|_{norm}=\frac{\partial|\lambda|}{\partial\alpha}\times\frac{\alpha}{|\lambda|} \tag{3.9}$$

Since $Z_m=\frac{1}{\lambda}$, thus

$$\left.\frac{\partial Z_m}{\partial\alpha}\right|_{norm}=-\frac{1}{\lambda^2}\frac{\partial|\lambda|}{\partial\alpha}\times\frac{\alpha}{|\lambda|} \tag{3.10}$$

Modal frequency sensitivity

$$\frac{df_m}{d\alpha} = \frac{\frac{\partial^2|\lambda|}{\partial f \partial \alpha}}{\frac{\partial^2|\lambda|}{\partial f^2}} \tag{3.11}$$

where

Z_m : modal impedance

f_m : harmonic resonance frequency

β : network component parameter

3.1.3 State-Space Model Based Method

One of those two noticeable methods based on modal analysis for harmonic resonance study is the state-space model based method [10]. In comparison with frequency scan analysis, the state-space model based method has overcome the restriction. By using the theory of modal analysis and sensitivity, the state space model based method can reveal the resonance points from the constructed transfer function; furthermore, network components influencing on harmonic resonances also are pointed out by using modal sensitivity [14]. The method consists of two techniques used in order to model the electric power system in state space that are called descriptor and *Y*(*s*) matrix.

The first technique, known as the descriptor, models the power system by using state-space equations as follows [13].

$$\dot{x} = Ax + bu \tag{3.12}$$

$$y = Cx \tag{3.13}$$

where:

x : the system variables are the capacitor voltages and inductor currents

u : input vector – harmonic source current

y : output vector – voltage

A, *b* and *C*: constant matrices. *A*: state space matrix

Applying the Laplace transformation, the system impedance is found as follow

$$X = (sI - A)^{-1} BU \tag{3.14}$$

$$Z(s) = \frac{y}{u} = C\frac{adj(sI - A)}{\det(sI - A)}B \tag{3.15}$$

$$Z_i(s) = \frac{1}{C_i}.\frac{\det(sI - A_i)}{\det(sI - A)} \tag{3.16}$$

where:

A_i : the matrix obtained from A after removing the row and column corresponding to V_i

C_i : the capacitance of the capacitor bank at bus i

The eigenvalue of the system impedance will reveal the series and parallel harmonic resonance points. This method allows identifying both resonance conditions in power systems; the eigenvalue and its sensitivity calculation in the manner with harmonic resonance mode analysis helps locate the most participated buses in resonance condition.

The second technique is known as $Y(s)$ matrix [14, 24]. The $Y(s)$ constructed as nodal admittance matrix in s – domain. Resonant frequencies are identified from the following equations

$$Y(s)x(s) = B.u(s) \tag{3.17}$$

$$y(s) = C.x(s) \tag{3.18}$$

$$Z(s) = \frac{y}{u} = C.Y(s)^{-1}.B \tag{3.19}$$

Thus

$$\left|Z(s)\right| = C.\left|Y(s)^{-1}\right|.B \tag{3.20}$$

The poles of the system revealing resonant frequencies are determined from the following equation.

$$det\left(Y(s)\right) = 0 \tag{3.21}$$

The sensitivity indices are also conducted in this approach in order to identify the most observable bus and network components influencing on harmonic resonance.

All in all, the advantages and disadvantages of each method listed above are summarized in Table 3.1 in following. The comparison points out that harmonic resonance mode analysis method is the most advanced method for harmonic resonance analysis. Therefore, this method is conducted in this study.

Table 3.1 Harmonic resonance analysis methods

	Frequency Scan Analysis	State Space Model Based Method	Harmonic Resonance Mode Analysis
Advantages	- Simple implementation. - Allow identifying possible harmonic resonances.	- Harmonic resonances are identified well. - The method provides information on the following issues during resonance condition: + The most observable bus. + The impact of network components on harmonic resonances.	- The method offers information on the following issues: + The severity of resonance between distinct resonant frequencies. + The most excitable and observable buses + The impacts of network components on
Disadvantages	- The method provides only information on resonant frequencies. - The method is time consuming because of the inverse of the admittance matrix [10].	- The information from the poles and zeros does not help to predict the severity of resonances between distinct resonant frequencies [10]. - The method is preferable to solve stability problems [10]. - There are some difficulties on modeling frequency dependent network parameters, especially model of distributed parameter line. - It is more complicated to construct A matrix when the size of electric power system is getting larger [25]. - To determine the poles of system is a complicated numerical task, especially using Y(s) matrix technique [10].	- There are different approaches to identify parallel and series resonance.

3.2 Modeling of Wind Power Plants

3.2.1 Reviews on Modeling of Wind Power Plants

Modeling of wind power plants plays an important role in harmonic assessment while the capacity of wind power plants is getting larger nowadays. A model of wind power plants needs to satisfy imperative requirements that are accuracy and time constraints. Many equivalent models of wind power plants have been proposed; however, some of these methods are still theoretical and need to be verified in practice [4, 26-29]. Generally, modeling wind power plants in harmonic assessment can be classified into two main groups in Figure. 3.3. as follows [30, 31].

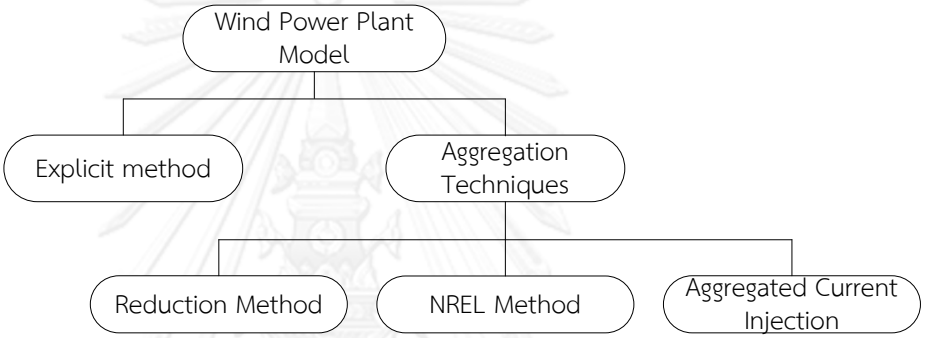

Figure 3.3 Summary of modeling of wind power plants

3.2.1.1 Explicit Model

The explicit model demonstrates all the wind turbine generators as complete and detailed models [4, 32, 33]. The method achieves considerable accuracy; nonetheless, the method requires a great amount of time on simulation. A sophisticated model still needs more investigation in order to achieve the objective of simulating the system manner well in harmonic assessment.

3.2.1.2 Aggregate Model

The aggregate model is becoming the noticeable trend in modeling wind power plants. The aggregate model allows simplifying analyses, and minimizing the simulation time. There are some pronounced aggregate methods in following.

The most simple aggregate model is based on IEC 61400-21, and IEC 61000-3-6 standards [2, 9]. The aggregate model represents wind power plants as harmonic current sources with or without the lumped capacitance at the collector [27]. The model is advantageous when considering connection compliance because of the simplicity. However, the model is limited in harmonic assessment, especially

harmonic resonance analysis because the impact of medium voltage system is totally neglected [27].

The other model of wind power plants mentioned is based on the reduction method [27]. The method is developed from two-port theory and dynamic transformation between two-port model and distributed parameter PI model that is used in modeling transmission lines [16]. The harmonic source is modeled as a harmonic current source, which matches accuracy significantly in comparison with the explicit model in calculation of individual harmonic voltage distortion. However, the disadvantage of the model is the shift of resonant frequencies, which can result in erroneous emission limit.

The last model is proposed by National Renewable Energy Laboratory (NREL) [34]. The model is based on the loss balance condition to construct an equivalent model. Wind power plants can be modeled including an equivalent transformer connected to the collector bus by the cable systems modeled as a PI model. The model has been validated by verifying with actual measurement data in power flow analysis, stability, harmonic emission and electromagnetic transient studies [35-37]. Although these studies have done for wind power plants in the range of 50 - 300 MW and provide good match with detail model in range of 0 – 2 kHz in harmonic emission study with type III wind turbines, conducting this model in harmonic resonance study is still worth considering. Details of this method will be summarized next. The validation among these aggregate models has been documented in [38] in light of field measurement verification.

The advantages and disadvantages of those methods listed above can be summarized in Table 3.2 in following. The comparison shows that NREL method is more advantageous than the others although some limitation still exists. Therefore, this study conducts NERL method for modeling of the wind power plant.

Table 3. 2. Summaries on advantages and disadvantages of those methods for modeling wind power plants

	Explicit Method	Aggregation Techniques		
		Current Injection	Reduction Method	NREL Method
Advantages	- Achieve good accuracy	- Simple implementation - Time saving simulation	- Acceptable accuracy - Simple implementation - Time saving simulation	- Good accuracy on stability, load flow, harmonic emission and transient studies. - Time saving simulation
Disadvantages	- Time consuming - Complicated implementation and numerical model	- Bad accuracy	- Shifts of resonant frequencies	- Provide good match with detail model in range 0-2 kHz in harmonic emission study for type III WTGs - Be applicable for wind power plant capacities of 50 – 300 MW.

3.2.2 Equivalent Model of Wind Power Plants

Wind power plants modeled in this study are based on the method proposed by National Renewable Energy Laboratory (NREL) [34]. The procedure of the method can be represented in Figure.3.4.

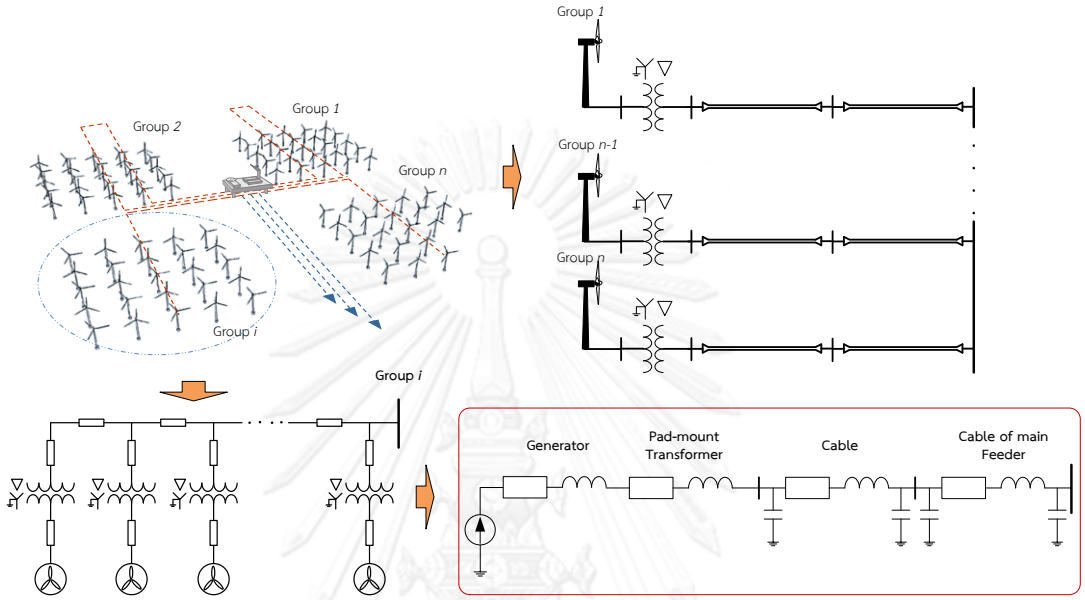

Figure 3.4 The procedure of equivalencing the wind power plant

The equivalent parameters of the model illustrated in Figure 3.4 calculated are based on an assumption that all wind turbine generators are assumed to inject currents with the same magnitude into system [26, 34]. The difference of phase angles of currents among wind turbine generators is neglected.

The following sections present in details how each equivalent parameter of each corresponding component in Figure 3.4 is calculated.

3.2.2.1 Equivalent Parameters of Main Feeders

Figure 3.5 illustrates the promising parameters for calculating those parameters of equivalent model for those main cables of feeders in the wind power plant.

The equivalent parameters of each feeder are calculated as

$$Z_{eq} = \frac{\sum_{i=1}^{n} Z_i m_i^2}{\left(\sum_{i=1}^{n} m_i\right)^2}; \quad B_{eq} = \sum_{i=1}^{n} B_i \tag{3.22}$$

Parameters of an equivalent model of the wind power plants are

$$Z_{eq} = \frac{\sum_{i=1}^{N} Z_{ieq} n_i^2}{\left(\sum_{i=1}^{N} n_i\right)^2}; \quad B_{eq} = \sum_{i=1}^{N} B_{ieq} \tag{3.23}$$

where:

m_i : the number of wind turbine generators in the *i*-th group.

Z_i and B_i : series impedance and shunt susceptance of each cable of the actual collector system.

n_i : the number of wind turbine generators in feeder *i*-th.

N : the number of feeders.

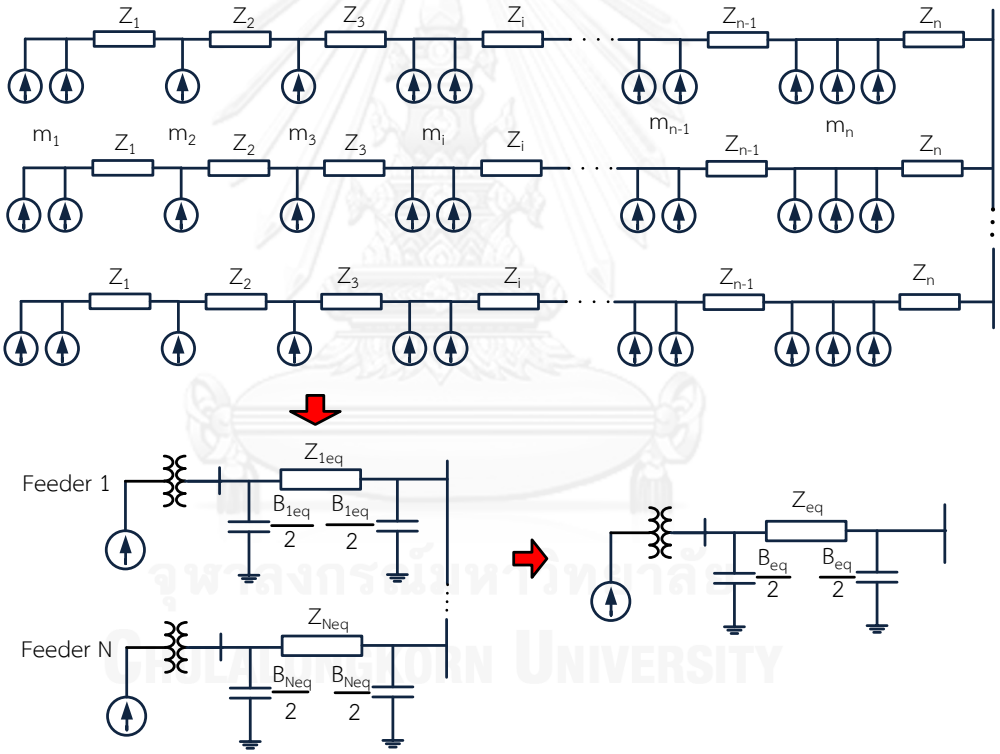

Figure 3.5 Equivalent model of a wind power plant

3.2.2.2 Equivalent Parameters of Remaining Components

The remaining components include cables, pad-mount transformers and wind turbine generators. These components are calculated by using the same procedure because of the similarity of position.

The cables, which connect between main platforms and pad-mount transformers, are taken as an example to calculate remaining components. Figure 3.6 represents the combination of all cables in an equivalent model.

$$Z_{eq} = \frac{Z_1 + Z_2 + ... + Z_n}{n}$$
$$B_{eq} = \sum_{i=1}^{n} B_i \qquad (3.24)$$

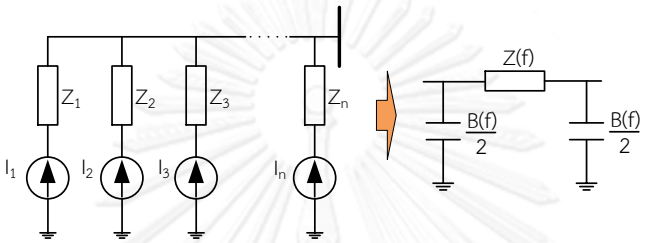

Figure 3.6 Equivalent parameters of cables connected between main feeders and pad-mount transformers

where:

Z_i and B_i : series impedance and shunt susceptance of each cable

n_i : the number of wind turbine generators in feeder *i*-th.

By analogy, those equivalent parameters of remaining components are also calculated by the equation (3.24).

CHAPTER IV

Problem Formulation and Solution

In this chapter, the problem is formulated and a methodology is represented as well in order to figure out how harmonic resonances are pointed out. The harmonic resonance mode analysis is conducted as core method in determining harmonic resonances. Harmonic models of network components are also presented in this chapter.

4.1 Problem Formulation

Harmonic resonances lead to high voltages or currents, which mainly result in high total voltage distortion. The study aims to analyze harmonic resonances well in term of voltage and current quality in accordance with standards. Harmonic resonance analysis is to identify potential harmonic resonances, and provide necessary information in order to support harmonic resonance mitigation. However, a harmonic resonance analyzing method is only considered validly when the results found in theory are valid in light of verification of field measurement. The problem in harmonic resonance analysis can be illustrated in Figure.4.1.

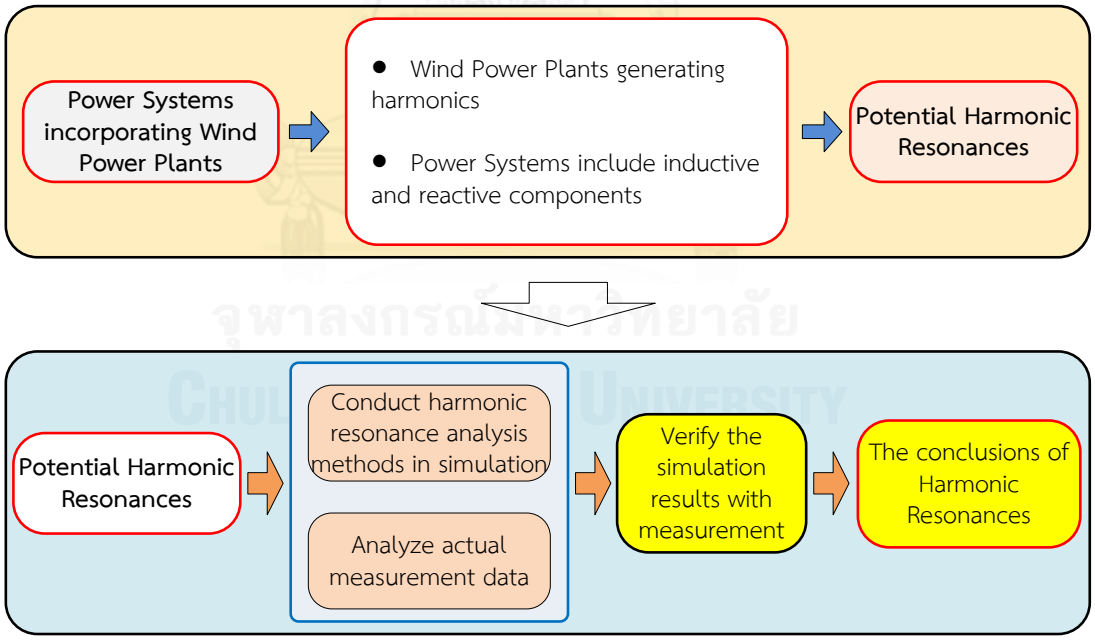

Figure 4.1 Problem formulation

4.2 Harmonic Modeling

Harmonic modeling of network components is a promising issue in harmonic study. The accuracy of used models affects directly reliability of simulation results.

Harmonic modeling of power systems is classified into two categories: harmonic sources and network components [39].

4.2.1 Supply Source Impedance

Supply source impedance is modeled as a series impedance in following:

$$Z_s = R_s + jhX_S \tag{4.1}$$

where: R_s, X_s are resistance and reactance calculated at fundamental frequency.

h is harmonic order.

4.2.2 Overhead Lines and Underground Cables

Overhead line and cable can be modeled as Pi or distributed parameter model (exact PI model) whose parameters are calculated at fundamental frequency. The normal PI model is usually applied for short line; however, the distributed parameter model is used when considering long line effect. The accuracy of each applied model depends on the length of overhead line and cable. The most significant difference between overhead line and underground cables is the shunt capacitance. As a result, the long line effect on cables is more significant than that on overhead lines [40].

The parameters of PI model, which is depicted in Figure.4.2, are calculated as follows.

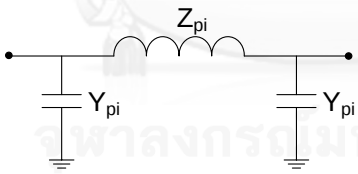

Figure 4.2 PI model

Normal PI model

$$\begin{aligned} Z_{pi} &= Z_{normal} = (R_0 + jhX_0)\ell \\ Y_{pi} &= Y_{normal} = jhB_0\ell / 2 \end{aligned} \tag{4.2}$$

Distributed parameter model

$$\gamma = \sqrt{2Z_{normal}Y_{normal}}$$
$$Z_{pi} = Z_{normal}\sinh(\gamma)/\gamma \quad (4.3)$$
$$Y_{pi} = Y_{normal}\tanh(\gamma/2)/(\gamma/2)$$

where:

R_0, X_0, B_0 : parameter of overhead line and cable (Ω/km, S/km)

ℓ : length of the overhead line and cable (km)

h : harmonic order

The skin effect is considered in simulation. Regarding the method proposed by Electricite de France (EDF) for overhead lines and cables at the voltage below 225 kV and harmonic order is above the second harmonic as follows [16].

Overhead line

At voltage 150; 90 kV

$$R = R_0\ell\left(1+\frac{0.646h^2}{192+0.518h^2}\right) \quad (4.4)$$

Cables

Voltage 150; 90 kV

$$R = R_0\ell(0.187+0.532\sqrt{h}) \quad (4.5)$$

4.2.3 Transformers

The classical model in [16] is used for modeling transformers in harmonic analysis. The model for single phase with no coupling between phases is represented simply as a short circuit impedance, which consists of frequency dependent parameters as in equation (4.6). The skin effect is incorporated in the harmonic model.

$$Z = R\sqrt{h} + jhX \quad (4.6)$$

where: R and X are resistance and reactance calculated at fundamental frequency

A sufficient harmonic model of a transformer needs to contain the following factors:

1. Magnetizing branch, in which transformers are taken into account as harmonic sources because of core saturation conditions [17, 41]. However, this issue is only included when transformers are main harmonic sources in power systems.

2. Capacitances of transformer windings should be taken into account of harmonic models when the area of analyzed frequency is up to 4 kHz

3. Transformer winding connection in Delta-Y also affects harmonic cancellation [17]. A phase shift of 300 in voltage needs to be included in the harmonic model.

4.2.4 Asynchronous Generators

The harmonic model of an asynchronous generator includes a resistance being connected in series with a reactance as [16, 42].

$$Z = R\sqrt{h} + jhX \tag{4.7}$$

where the reactance is calculated in case of locked rotor; the sum of rotor and stator reactances is the equivalent reactance.

4.2.5 Synchronous Generators

It is similar equation in (4.7) to calculate the parameters of harmonic model used for asynchronous generators. However, the resistance is calculated from the power losses of the machine, and the reactance is the sub-transient reactance [16]

4.3 Solution Method

The solution method is depicted in Figure.4.3.

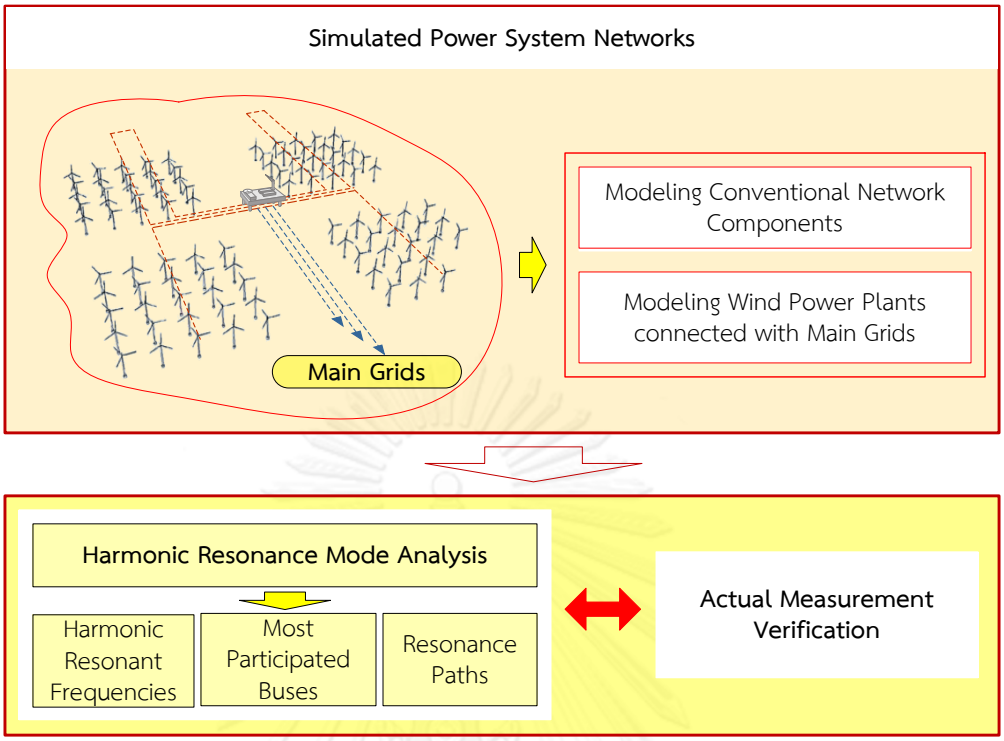

Figure 4.3 Solution Method

As discussed in chapter 3 part 3.1, reviews on harmonic resonance analyses show that harmonic resonance mode analysis method brings more advantages in resonance study than other methods. Harmonic resonance mode analysis not only points out possible resonances but also provide necessary information to harmonic mitigation when those most participated buses and resonance paths are determined during resonances.

However, the simulation results found by using harmonic resonance mode analysis need to be verified with actual measurement data in order to validate the method applied. The verification results worked out help clarify two following points:

1. Applicability of harmonic resonance mode analysis
2. Validity of the model of the wind power plant in harmonic resonance study

Harmonic resonance mode analysis has been presented in chapter 3, nonetheless, those details of this method have not documented well. The following parts will present elaborately this method and the procedure of actual measurement verification as well.

4.3.1 Harmonic Resonance Mode Analysis

As harmonic resonance mode analysis has been partially documented previously; the most important information is presented as well. The following is those details of this method.

The key of harmonic resonance mode analysis technique is to determine the smallest eigenvalue of network admittance matrix that is named as critical eigenvalue. Those promising indices in the technique are illustrated in Figure. 4.4 as follows.

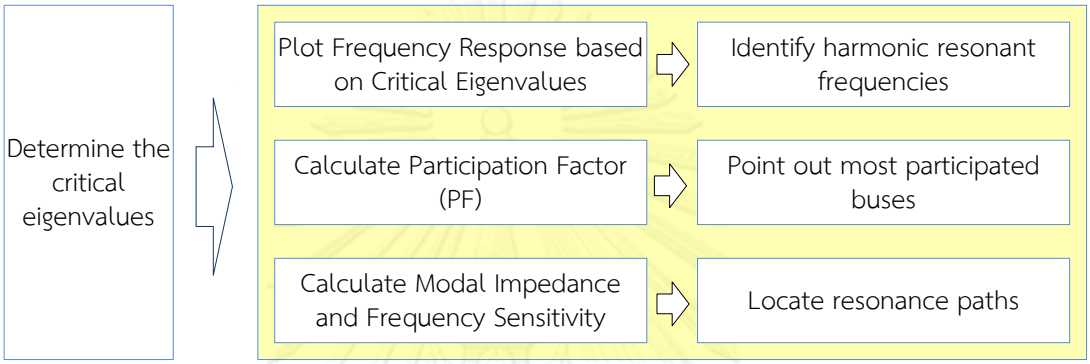

Figure 4.4 Diagram of calculating indices in harmonic resonance mode analysis

The critical eigenvalues are calculated as

$$[V]_f = [Y]_f^{-1}[I]_f \tag{4.8}$$

$$[Y]_f = [L]_f[\Lambda]_f[T]_f \tag{4.9}$$

where

$[Y]_f$: the system admittance matrix at harmonic frequency f,

$[V]_f$ and $[I]_f$: the node voltage and nodal current injection respectively.

L (= $[l_1, l_2,\ldots,l_n]$) and T (= $[t_1, t_2,\ldots, t_n]$)^T : the left and right eigenvector $[L] = [T]^{-1}$. Super script T demonstrates matrix transpose.

$[\Lambda]$: the diagonal admittance matrix with eigenvalues $\lambda_1,\ldots,\lambda_n$

$$[\Lambda] = \begin{bmatrix} \lambda_1 & 0 & \ldots & 0 \\ 0 & \lambda_2 & . & 0 \\ 0 & . & \ldots & 0 \\ 0 & 0 & \ldots & \lambda_n \end{bmatrix}$$

The modal impedance matrix is obtained by the inverse of $[\Lambda]$. By defining $[U] = [T][V]$ or $[V] = [T]^{-1}[U] = [L][U]$ and $[J] = [T][I]$, equation (4.9) is rewritten as

$$[V] = [L][\Lambda]^{-1}[T][I] \tag{4.10}$$

$$[T][V] = [\Lambda]^{-1}[T][I] \tag{4.11}$$

$$[U] = [\Lambda]^{-1}[J] \tag{4.12}$$

The inverse of the smallest eigenvalue at each certain harmonic frequency is called modal impedance. The curve of modal impedance with corresponding harmonic frequencies plotted helps identify the harmonic resonance points at the peaks of this curve. This curve is illustrated in Figure. 4.5 as below [15].

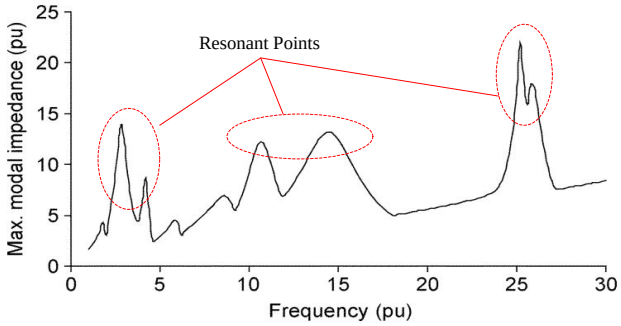

Figure 4.5 Frequency scan based on harmonic resonance mode analysis technique

Without loss of generality, λ_1 is assumed to be the smallest eigenvalue of admittance matrix at a certain harmonic frequency *f*. The promising indices are calculated corresponding λ_1 as.

Participation factors (*PF*):

Equation (4.10) can be derived in following as λ_1 is the smallest eigenvalues [15].

$$[V] = [L]\begin{bmatrix} \lambda_1^{-1} & 0 & \dots & 0 \\ 0 & \lambda_2^{-1} & . & 0 \\ 0 & . & \dots & 0 \\ 0 & 0 & \dots & \lambda_n^{-1} \end{bmatrix}[T][I] \simeq [L]\begin{bmatrix} \lambda_1^{-1} & 0 & \dots & 0 \\ 0 & 0 & . & 0 \\ 0 & . & \dots & 0 \\ 0 & 0 & \dots & 0 \end{bmatrix}[T][I] =$$

$$= \begin{bmatrix} \lambda_1^{-1} L_{11} & 0 & \dots & 0 \\ \lambda_1^{-1} L_{21} & 0 & \dots & 0 \\ \dots & \dots & 0 & \dots \\ \lambda_1^{-1} L_{n1} & 0 & \dots & 0 \end{bmatrix} \begin{bmatrix} T_{11} & T_{12} & \dots & T_{1n} \\ T_{21} & T_{22} & \dots & T_{2n} \\ \dots & \dots & T_{ij} & \dots \\ T_{n1} & T_{n2} & \dots & T_{nn} \end{bmatrix} [I]$$

$$= \lambda_1^{-1} \begin{bmatrix} L_{11}T_{11} & L_{11}T_{12} & \dots & L_{11}T_{1n} \\ L_{21}T_{21} & L_{21}T_{22} & \dots & L_{21}T_{2n} \\ \dots & \dots & L_{i1}T_{ij} & \dots \\ L_{n1}T_{n1} & L_{n1}T_{n2} & \dots & L_{n1}T_{nn} \end{bmatrix} [I] \quad (4.13)$$

The main diagonal line of matrix derived in equation (4.13) includes participation factors. The largest element identifies the largest participation factor, which is used to figure out the most participated bus during resonance. As derived in (4.13), the participation factors can be calculated by product of corresponding elements of the left and right eigenvectors . Generally, the participation factor can be calculated as.

$$PF = L_{bm} T_{mb} \quad (4.14)$$

where

PF : participation factor

L_{mb} & T_{bm} : elements of left and right eigenvectors that correspond to mode m and bus b

Modal impedance and frequency sensitivity indices and resonance paths:

As chapter 3 part 3.1:

Modal impedance sensitivity

$$\left.\frac{\partial \lambda}{\partial \alpha}\right|_{norm} = \frac{\partial |\lambda|}{\partial \alpha} \times \frac{\alpha}{|\lambda|} \quad (4.15)$$

Since $Z_m = \frac{1}{\lambda}$, thus

$$\left.\frac{\partial Z_m}{\partial \alpha}\right|_{norm} = -\frac{1}{\lambda^2} \frac{\partial |\lambda|}{\partial \alpha} \times \frac{\alpha}{|\lambda|} \quad (4.16)$$

Modal frequency sensitivity

$$\frac{df_m}{d\alpha} = \frac{\frac{\partial^2|\lambda|}{\partial f \partial \alpha}}{\frac{\partial^2|\lambda|}{\partial f^2}} \tag{4.17}$$

where α is a network component, f_m is a resonant frequency.

Based on those indices calculated, the method provides a scheme of harmonic mitigation in Figure.4.6 if harmonic resonances are possible.

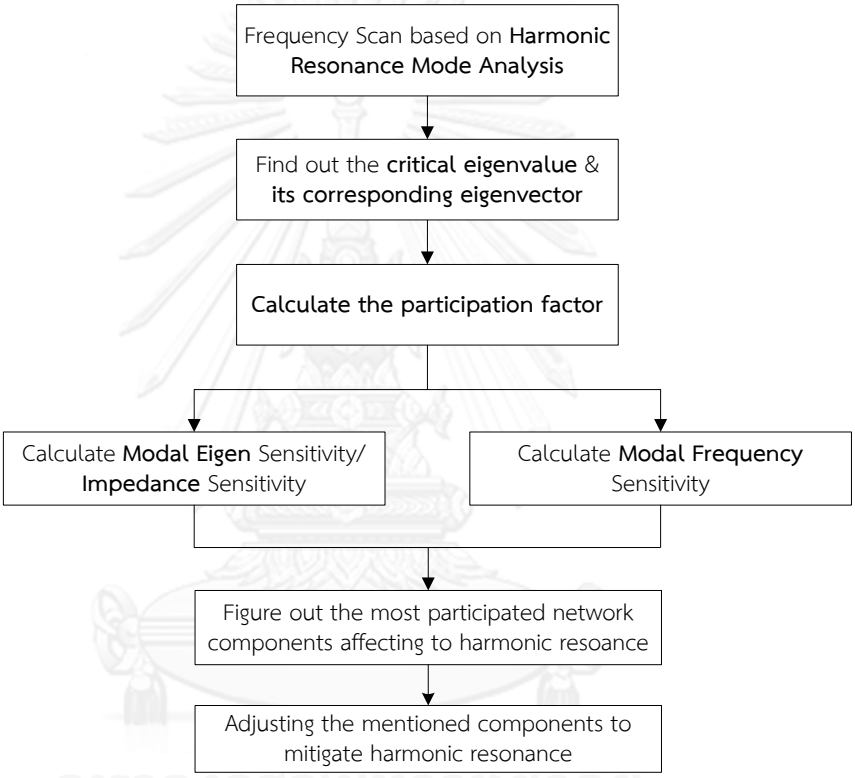

Figure 4.6 Harmonic resonance mitigation scheme [22]

Both modal impedance and frequency sensitivity indices are used to point out most participated network components into resonances as in Figure 4.6. There is a slight difference between these indices in light of their sensitivity to variation of resonant frequency [22]. The modal frequency sensitivity index is more sensitive to the change of network component parameter in term of the shift of resonant frequencies while model impedance sensitivity relates mostly to the variation of magnitude of frequency response of the system. However, both indices cooperate with each other in identifying those components affecting mainly resonances. In other word, the goal of mitigating harmonic resonances can be caught by using these indices.

Furthermore, these indices are also used to define resonance paths in following.

Resonance Paths

Resonance paths can be defined as an area that includes those most participated network components in resonances, which are figured out by sensitivity indices.

As the scheme is shown in Figure 4.7, those most participated network components are used to construct resonance paths that provide crucial information on adjustment of network parameters in avoiding resonances. In other words, resonance paths provide a full picture about harmonic resonance propagation through power systems. Figure 4.7 illustrates a resonance path in a simple distribution network.

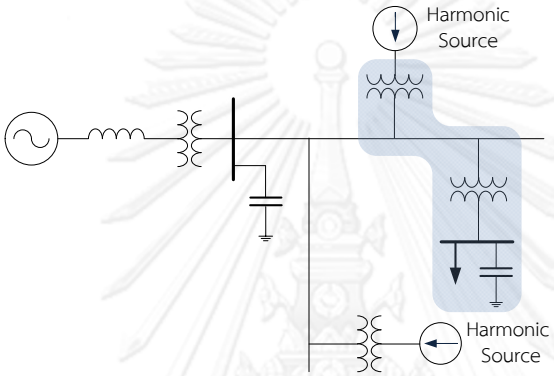

Figure 4.7 A resonance path in a simple network

4.3.2 Verification Procedure

The simulation results found by using harmonic resonance mode analysis technique are verified with actual measurement data. The actual measurement data analyzed are based on the procedure that is illustrated in Figure 4.8 below.

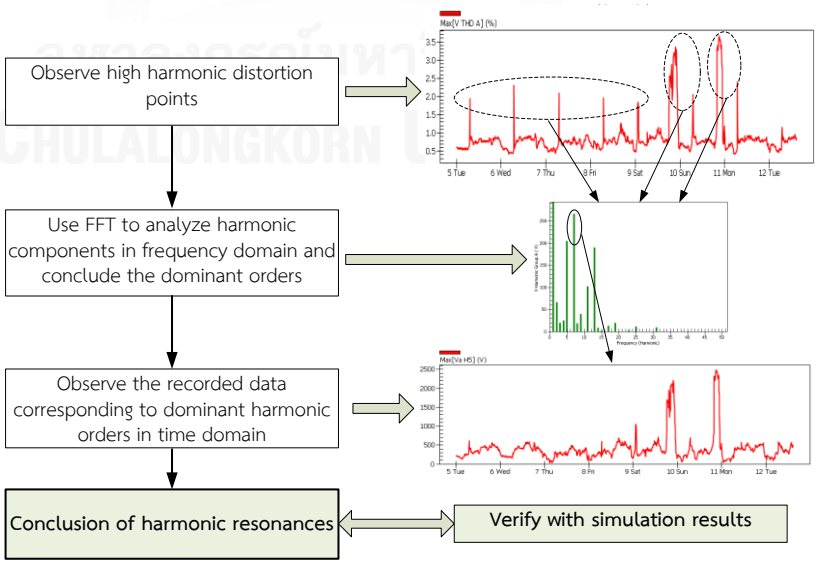

Figure 4.8 Verification procedure

Parallel resonance is considered as a main phenomenon in this study. As mentioned previously, harmonic resonance leads to very high harmonic voltage distortion. Consequently, based on this characteristic, harmonic resonances are detected when analyzing actual measurement data. Observing the high harmonic total distortion helps predict skeptical points of resonances. The skeptical points corresponding to a certain recorded time will be analyzed in frequency domain by using Fast Fourier Transform (FFT) in order to figure out dominant harmonics. These dominant harmonics will be considered against time domain to give conclusion of resonance. The conclusion is used to verify the simulation results.

CHAPTER V

Test Results and Analysis

In chapter 5, the proposed method is applied to the test system, which is the first wind farm in Thailand. Simulation results are then verified with the actual measurement data, which is based on the procedure of verification proposed in chapter IV.

5.1 Test Result

Harmonic resonance mode analysis (HRMA) method is applied to the test system, which is described in details in chapter IV. Wind power plants modeled by using NERL method will be considered for two cases. The former model includes entirely network components that is called an equivalent of complete collectors (EOCC), and only the main cables of feeders are modeled in latter one, which is named as an equivalence of main lines (EOML) [26, 34].

5.1.1 Simulated Power System

The test system used in the study is the first wind power plant in Thailand, which is located in Nakorn Rachasrima province in Northeastern part of Thailand. The wind power plant has capacity of 90 MW consisting of 45 wind turbine generators with rated power of 2.3 MW each. All wind turbine generators are equipped in the wind power plant are full rated converter induction generator type IV with terminal voltage of 690 V. The wind power plant is connected to medium voltage system by 45 pad-mount transformers and underground cables 33 kV. The power from wind power plant is transmitted to the main grid through two step-up transformers 33/115 kV at the substation and 115 kV transmission overhead line system. The tie circuit breaker at 33 kV bus bar is operated as normally open (NO).

There are four meters (M1, M2, M3 and M4) equipped in the wind power plant and high voltage system. The procedure of measurement is in accordance with IEC 61400-21standard [9]. The data were collected in 8 days from 5th of March to 13th of March 2013 with 10-minute average data recorded. All the collected data were handled by using MATLAB software for harmonic analysis.

The main configuration of wind turbines used in the wind farm is illustrated in Figure 5.1. Main components of the wind farm and the system configuration with the meter location are described in Figures 5.2 and 5.3 respectively. A single line impedance of the test system is illustrated in Figures 5.4 and 5.5.

Table 5.1 Number of wind turbine generators (WTGs) in the test system

Feeder 1		Feeder 2		Feeder 3		Feeder 4		Feeder 5	
WTGs	11	WTGs	7	WTGs	9	WTGs	11	WTGs	7
MW	25.3	MW	16.1	MW	20.7	MW	25.3	MW	16.1

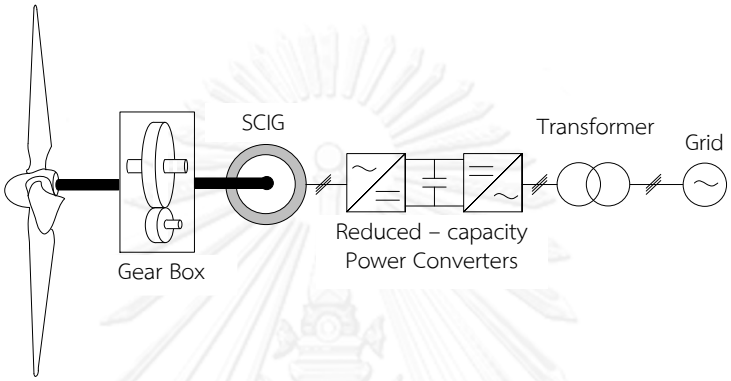

SCIG: Squirrel Cage Induction Generator

Figure 5.1 The configuration of wind turbines

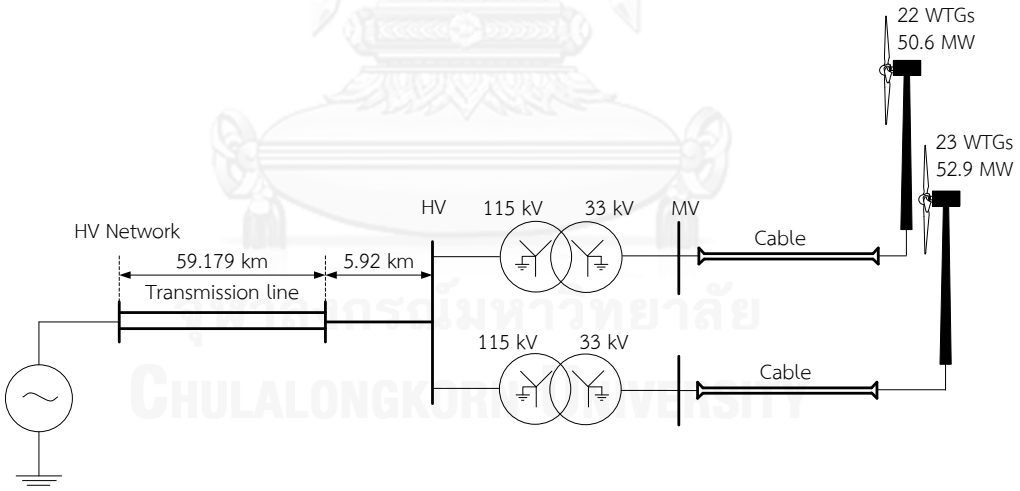

Figure 5.2 Main components of the wind farm

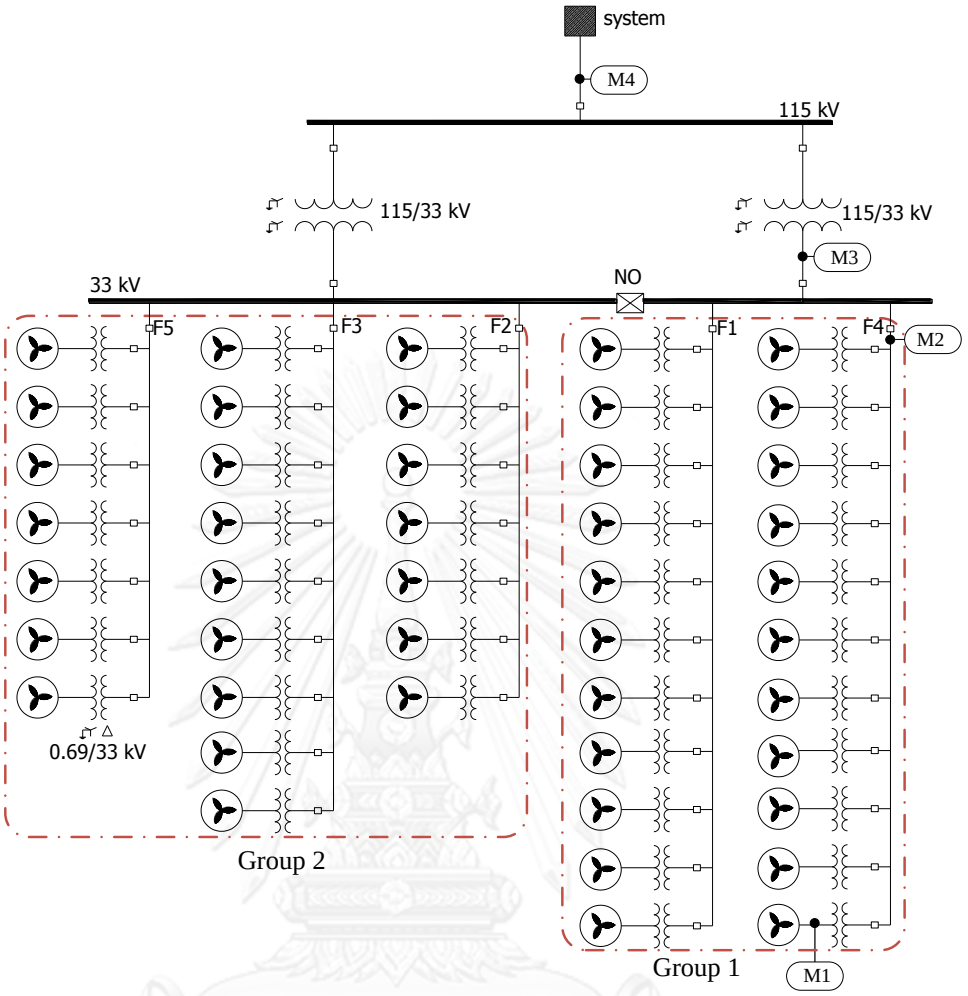

Figure 5.3 Single diagram of test system

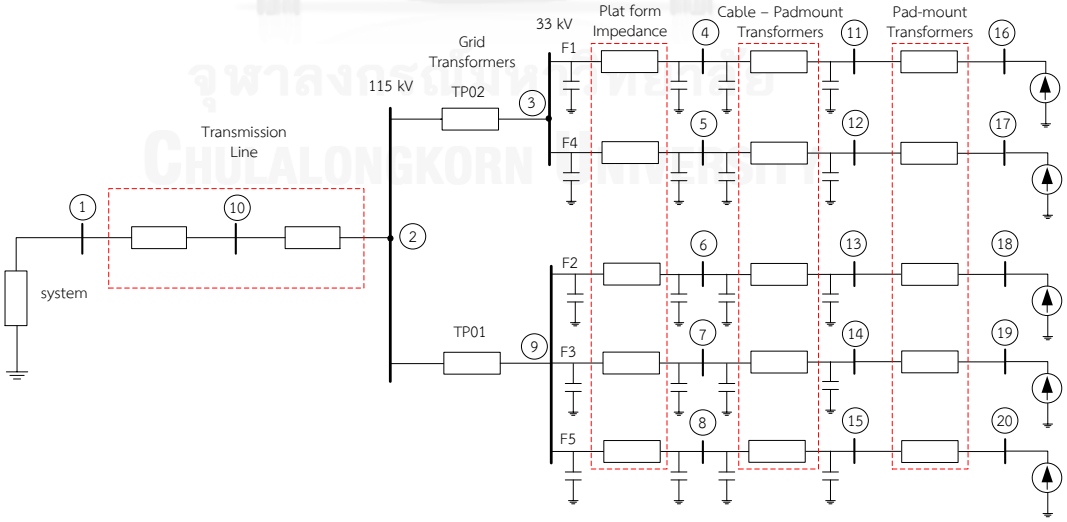

Figure 5.4 The single phase impedance of test system modeled by using EOCC

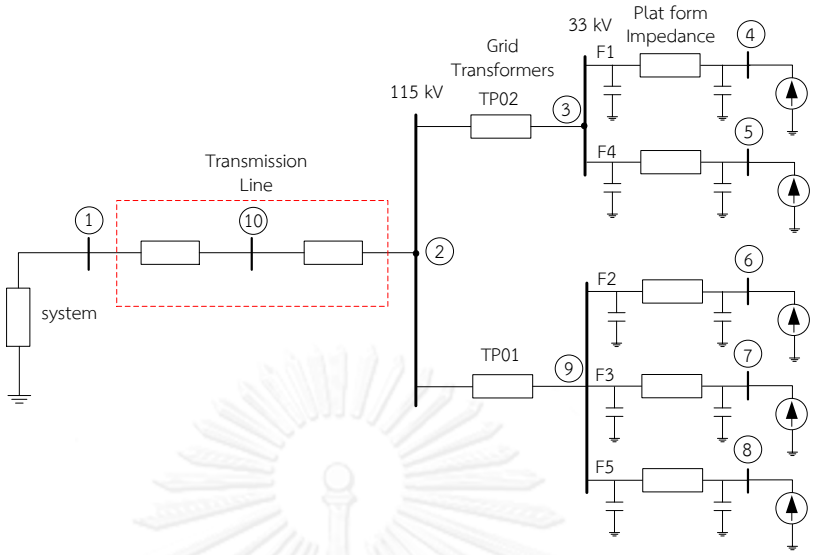

Figure 5.5 The single phase impedance of test system modeled by using EOML

5.1.2 Simulation Results

Two scenarios are considered in simulation. The first scenario is in full operation of wind turbine generators, and only group 1 or group 2 is taken into account in the second scenario. The 115 kV bus is the point of common coupling (PCC) bus, and 33 kV bus is the collector bus of the wind power plant. Therefore, these buses are considered mainly in the simulation.

The scenarios are considered in different operation of the wind power plant, which helps point out the possible harmonic resonances in the system. The influences of network components on harmonic resonances also are evaluated by using sensitivity indices. The variation of resonant frequencies is recorded to assess the impacts of the wind farm's operation on the applicability of harmonic resonance mode analysis.

5.1.2.1 Scenario 1

The first scenario considers full wind turbine generators in operation. Both EOML and EOCC are used in modeling the wind power plants in order to evaluate the influence of entire wind power plants on the accuracy of identifying harmonic resonances.

Simulation results found by using harmonic resonance mode analysis are presented in Table 5.2.

Table 5.2 Results of modal frequency scan analysis with EOCC model of the wind power plant

Resonant Frequency (P.U)	Critical mode	Critical Eigenvalue	Modal Impedance	Participation Factor (P.U)	Most Part.Bus	Least Part.Bus
6	1	0.0008	1217.593	0.0542	19	1
16.4	1	0.0008	1265.671	0.0716	16	2
19.4	1	0.0017	585.8302	0.0908	16	2
45.8	1	0.009	110.5709	0.1668	16	9
47.5	20	0.0069	145.2056	0.1869	20	10

Table 5.3 Results of modal frequency scan analysis with EOML model of the wind power plant

Resonant Frequency (P.U)	Critical mode	Critical Eigenvalue	Modal Impedance	Participation Factor (P.U)	Most Part.Bus	Least Part.Bus
6.7	10	0.0012	869.0115	0.1178	8	1
18.5	10	0.0016	624.2397	0.1826	4	2
23.7	1	0.0038	262.6373	0.2706	1	2

* Most Part.Bus – Most Participated Bus Least Part.Bus – Least Participated Bus

The frequency response of the system derived from modal frequency scan analysis is illustrated in Figure 5.6. Furthermore, frequency scan analysis is also conducted at 115 kV and 33 kV buses corresponding to bus 2 and 3, 9 respectively in Figure 5.5. Frequency responses at these buses are depicted in Figures 5.6 and 5.7.

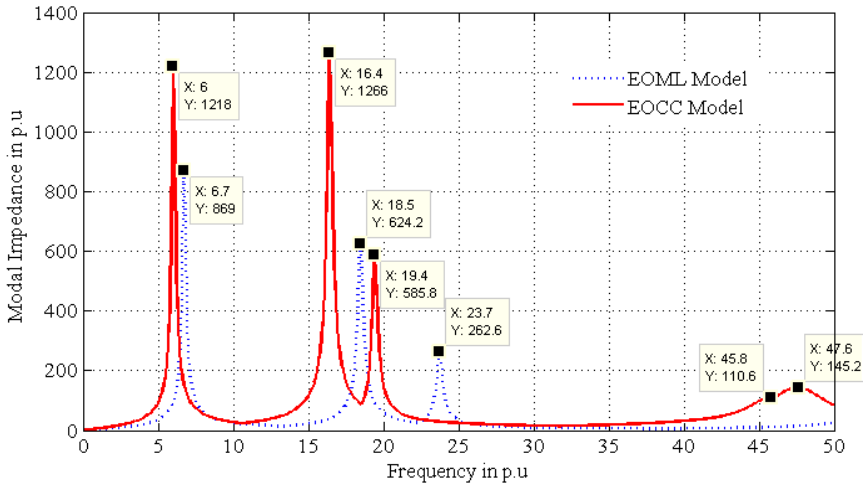

Figure 5.6 The frequency response of the test system

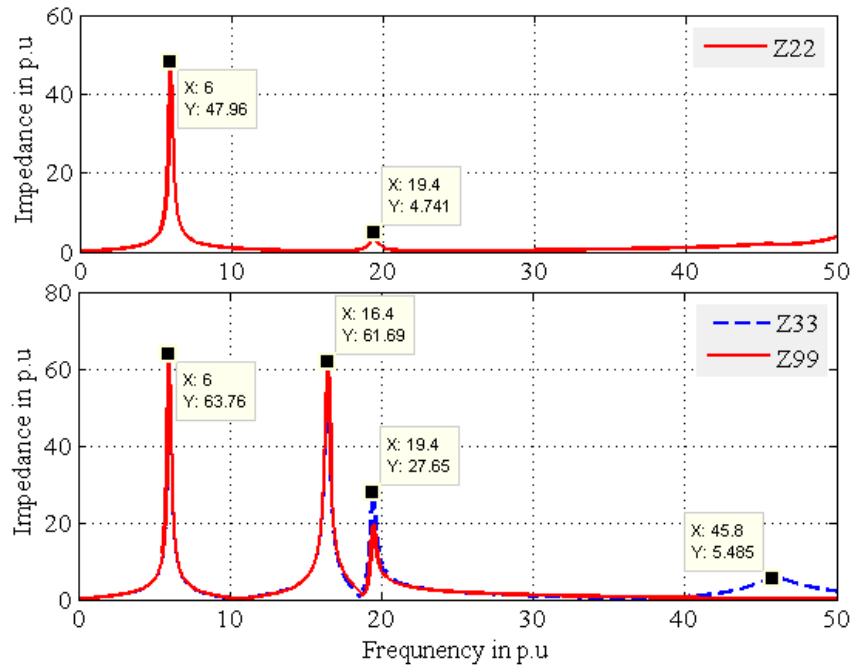

Figure 5.7 Frequency scan analysis conducted at 115 kV and 33 kV buses

The frequency response in Figure 5.6 shows that harmonic resonant frequencies found with EOML of the wind power plant are close to resonant frequencies in complete model of the wind power plant. The results indicate that harmonic resonances tend to happen in the area of low frequency. Therefore, from the Figures 5.6 and 5.7, it reveals that harmonic resonances potentially happen between 5th and 6th harmonics, and between 19th and 20th harmonics at both 115 kV and 33 kV buses.

There is only a resonance happening between 16th and 17th harmonics at 33 kV bus, and another resonance is potential to happen between 45th and 46th harmonics. However, frequency scan based on modal analysis indicates that the amplification of the resonance between 45th and 46th harmonic frequencies is insignificant, which is also observed at frequency scan analysis at 33 kV bus.

To point out the most participated bus and locate the resonance paths in harmonic resonance, calculating the sensitivity indices are necessary. Modal eigen - sensitivity or modal impedance and frequency sensitivity indices are tabulated in Tables 5.4-5.13, those graphs presenting these indices are plotted in Figures 5.8 - 5.17.

- At resonant frequency h = 6

The eigen and frequency sensitivity indices are tabulated in Tables 5.4-5.5. Those graphs of these indices are shown in Figures 5.8 – 5.9 respectively.

Table 5.4 Eigen sensitivity at h = 6

No.	Components - α	$\frac{\partial\lambda}{\partial\alpha}$(%)
1	System resistance	-1029.67
2	Transformer reactance branch 2-9	-841.333
3	Transformer reactance branch 2-3	-663.262
4	Transformer resistance branch 2-9	-124.558
5	Transmission line resistance branch 1-10	-101.826
6	Transformer resistance branch 2-3	-92.8288
7	Transmission Line reactance branch 2-10	-54.9276
8	System reactance	28.4069
9	Transmission line reactance branch 1-10	3.7122
10	Transmission line resistance branch 2-10	-0.9713

Table 5.5 Frequency sensitivity at h = 6

No.	Components - α	$\frac{\partial f}{\partial \alpha}(\frac{rad}{100\%})$
1	Transformer reactance branch 2-9	38.3559
2	Transformer reactance branch 2-3	29.7974
3	System reactance	-13.4265
4	Transmission Line reactance branch 2-10	-4.2521
5	System resistance	2.9358
6	Transmission line reactance branch 1-10	-1.3268
7	Transformer resistance branch 2-9	-0.8045
8	Transmission line reactance branch 1-10	-0.6273
9	Transformer resistance branch 2-3	0.4835
10	Line charging transmission line branch 2-10	0.0148

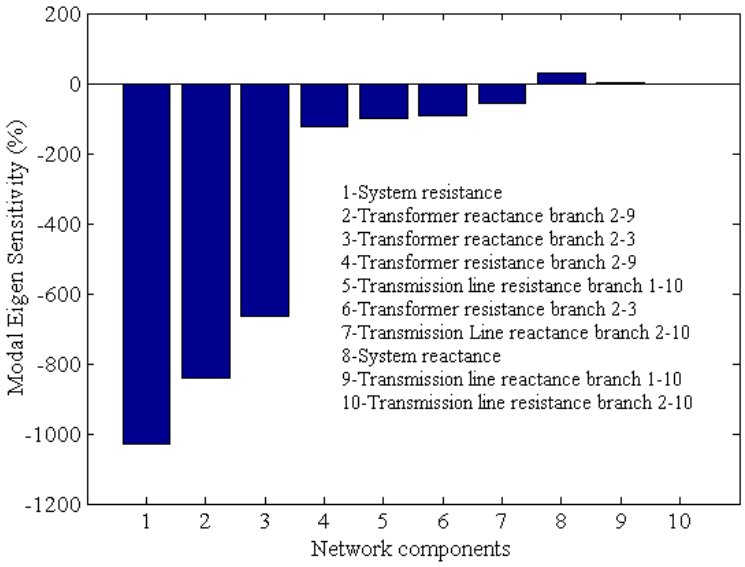

Figure 5.8 Eigen-sensitivity at h = 6

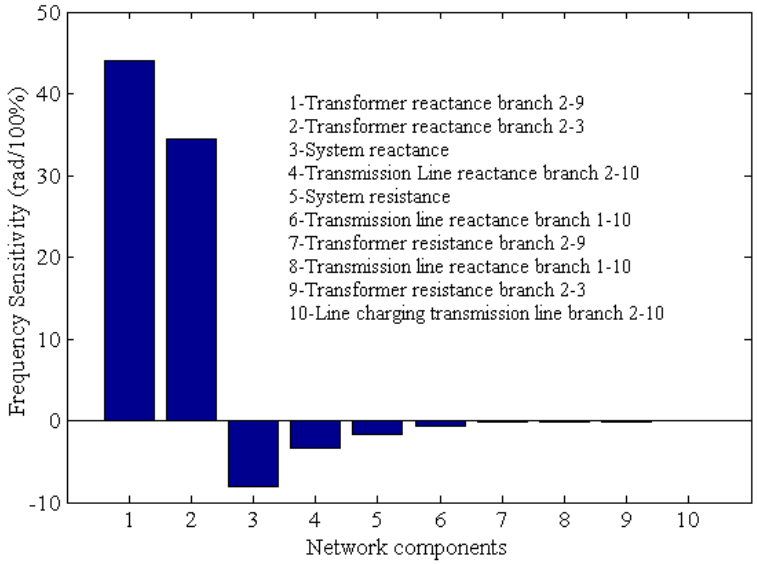

Figure 5.9 Frequency sensitivity at h = 6

There is a small difference in the order of the most sensitivity network components affecting harmonic resonance at the 6th harmonic. The frequency sensitivity indices seem to be reasonable when the most participated component in harmonic resonance is reactance of the step up transformers while the system resistance is pointed out in calculation of eigen - sensitivity. Basically, resistance is commonly known as a damping factor, and resistance and capacitance are main origins in harmonic resonance. As a result, the calculation in Tables 5.4 and 5.5 and those graphs in Figures 5.8 and 5.9 partially show theoretically impacts of network components on the harmonic resonance. Generally, both sensitivity indices are quite compatible in calculation with respect to first five network components. Transformer and transmission line affect mainly harmonic resonance while the wind power plant does not contribute any component to consideration of factors influencing on the harmonic resonance. In other words, a few adjustments of main grid components can results in significantly harmonic resonant frequencies in the system

- At resonant frequency h = 16.4

The eigen and frequency sensitivity indices are tabulated in Tables 5.6-5.7. Those graphs of these indices are shown in Figures 5.10 – 5.11 respectively.

Table 5.6 Eigen sensitivity at h = 16.4

No.	Components - α	$\frac{\partial \lambda}{\partial \alpha}$(%)
1	Transformer reactance branch 2-9	-43235
2	Transformer reactance branch 2-3	-34565
3	Transformer resistance branch 2-9	1739.77
4	Transformer resistance branch 2-3	1462.31
5	Equivalent resistance of main cable feeder 1	-65.915
6	Equivalent resistance of main cable feeder 3	-29.516
7	Equivalent resistance of main cable feeder 5	-19.199
8	Equivalent reactance of main cable feeder 1	-8.7698
9	Equivalent resistance of main cable feeder 4	-7.8966
10	System resistance	-7.4853

Table 5.7 Frequency sensitivity at h = 16.4

No.	Components - α	$\frac{\partial f}{\partial \alpha}(\frac{rad}{100\%})$
1	Transformer reactance branch 2-9	-847.06
2	Transformer reactance branch 2-3	-696.09
3	Transformer resistance branch 2-9	-29.665
4	Transformer resistance branch 2-3	-24.035
5	Equivalent resistance of main cable feeder 1	0.8496
6	Equivalent resistance of main cable feeder 3	0.3799
7	Equivalent resistance of main cable feeder 5	0.2469
8	Transmission Line reactance branch 2-10	-0.1633
9	Equivalent reactance of main cable feeder 1	0.1589
10	System reactance	0.1083

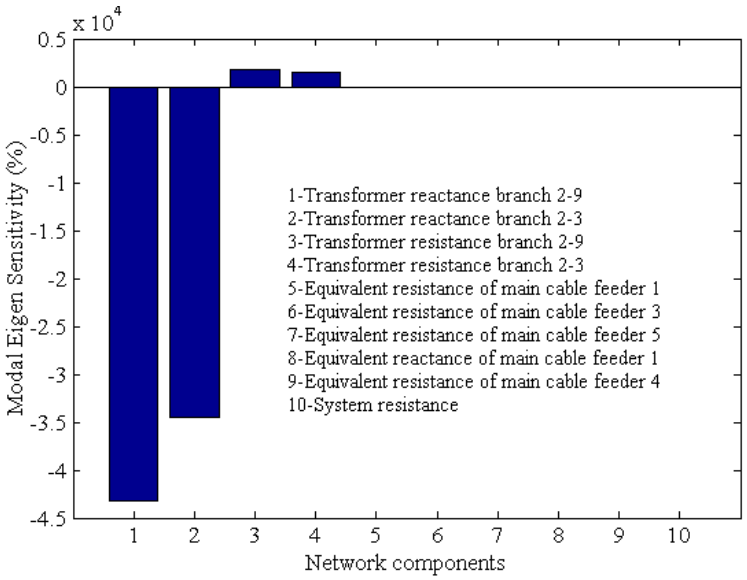

Figure 5.10 Eigen-sensitivity at h = 16.4

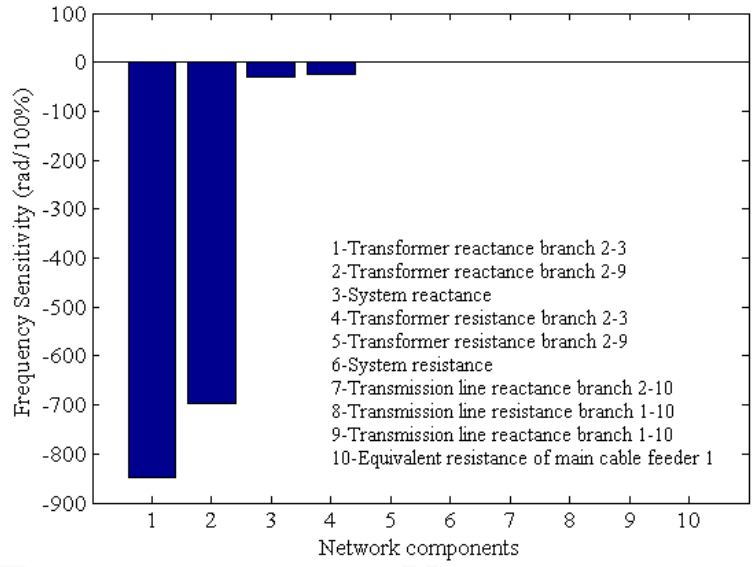

Figure 5.11 Frequency sensitivity at h = 16.4

As shown in Tables 5.6 and 5.7 and those graphs in Figures 5.10 and 5.11, main grid components still play an important role in considering influences on the resonance between the 16th and 17th harmonics. However, some equivalent components of the wind power plants also impact on the harmonic resonance in this case.

- At resonant frequency h = 19.4

The eigen and frequency sensitivity indices are tabulated in Tables 5.8 - 5.9. Those graphs of these indices are shown in Figures 5.12 – 5.13 respectively.

Table 5.8 Eigen sensitivity at h = 19.4

No.	Components - α	$\frac{\partial \lambda}{\partial \alpha}$(%)
1	Transformer reactance branch 2-3	-30398
2	Transformer reactance branch 2-9	-22611
3	System reactance	-1409.8
4	Transformer resistance branch 2-3	1299.49
5	Transformer resistance branch 2-9	1098.34
6	System resistance	-905.41
7	Transmission line reactance branch 2-10	-770.16
8	Transmission line resistance branch 1-10	-327.86
9	Transmission line reactance branch 1-10	-211.24
10	Equivalent resistance of main cable feeder 1	-76.248

Table 5.9 Frequency sensitivity at h = 19.4

No.	Components - α	$\frac{\partial f}{\partial \alpha}(\frac{rad}{100\%})$
1	Transformer reactance branch 2-3	-1135.2
2	Transformer reactance branch 2-9	-875.22
3	Transmission line reactance branch 2-10	-47.933
4	Transformer resistance branch 2-3	19.324
5	Transformer resistance branch 2-9	15.2397
6	System reactance	-10.286
7	System resistance	-9.0344
8	Transmission line resistance branch 1-10	-2.1662
9	Transmission line reactance branch 1-10	-1.8608
10	Equivalent resistance of main cable feeder 1	-0.8884

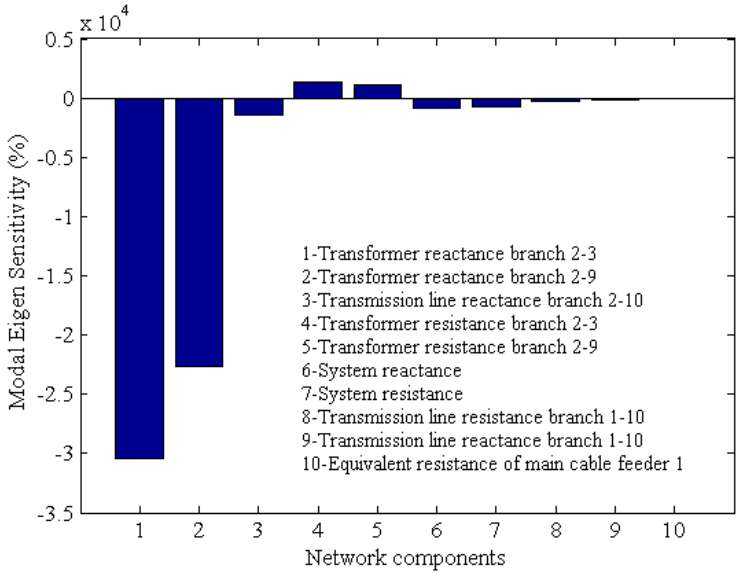

Figure 5.12 Eigen-sensitivity at h = 19.4

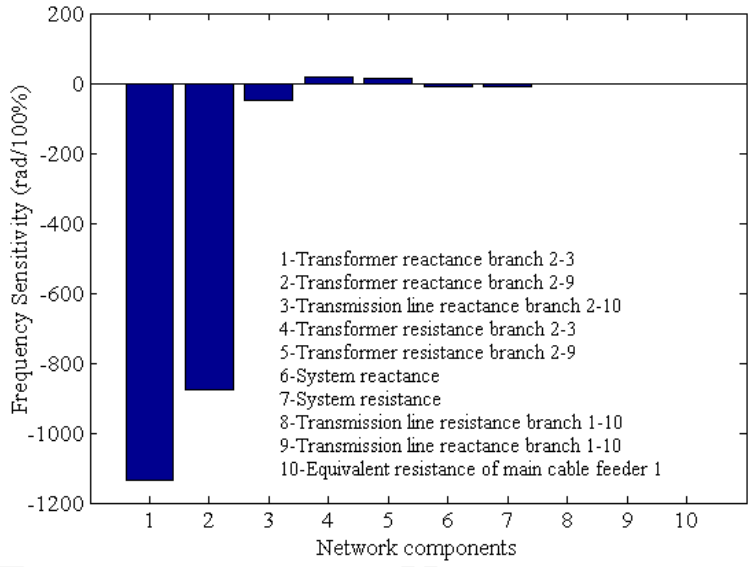

Figure 5.13 Frequency sensitivity at h = 19.4

Similarly what observed at resonant frequency of the 6th order, both sensitivity indices calculated in Tables 5.8 and 5.9 are quite consistent. Most participated network components in harmonic resonances are transformer and transmission line reactance, which is pointed out by both sensitivity indices.

- **At resonant frequency h = 45.8**

The eigen and frequency sensitivity indices are tabulated in Tables 5.10 - 5.11 Those graphs of these indices are shown in Figures 5.14 – 5.15 respectively.

Table 5.10 Eigen sensitivity at h = 45.8

No.	Components - α	$\frac{\partial\lambda}{\partial\alpha}$(%)
1	Equivalent resistance of main cable feeder 1	-690.17
2	Equivalent reactance of main cable feeder 1	-540.49
3	Transmission Line reactance branch 1-10	-279.77
4	Transformer reactance branch 2-3	-170.12
5	Equivalent resistance of main cable feeder 4	-103.82
6	Equivalent reactance of main cable feeder 4	-64.371
7	System reactance	-52.452
8	Transformer reactance branch 2-9	-49.303
9	Transformer resistance branch 2-3	20.4507
10	Equivalent resistance of main cable feeder 3	-4.8682

Table 5.11 Frequency sensitivity at h = 45.8

No.	Components - α	$\frac{\partial f}{\partial\alpha}(\frac{rad}{100\%})$
1	Transformer reactance branch 2-3	-202.47
2	Equivalent reactance of main cable feeder 1	55.4969
3	Transformer reactance branch 2-9	-44.577
4	Equivalent reactance of main cable feeder 4	11.2807
5	Transmission Line reactance branch 1-10	7.99
6	Equivalent line charging of main cable feeder 1	-2.4985
7	Equivalent resistance of main cable feeder 1	-1.6324
8	Transmission line reactance branch 2-10	-1.1822
9	System reactance	1.0824
10	Equivalent resistance of main cable feeder 3	0.6938

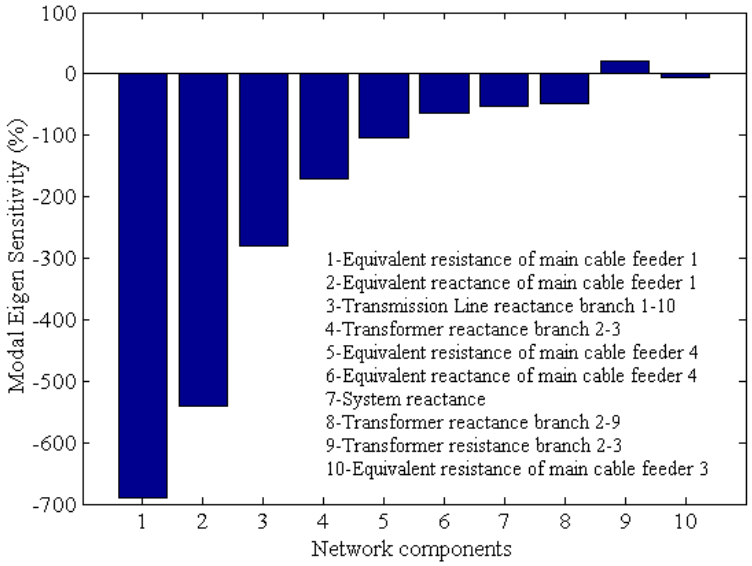

Figure 5.14 Eigen-sensitivity at h = 45.8

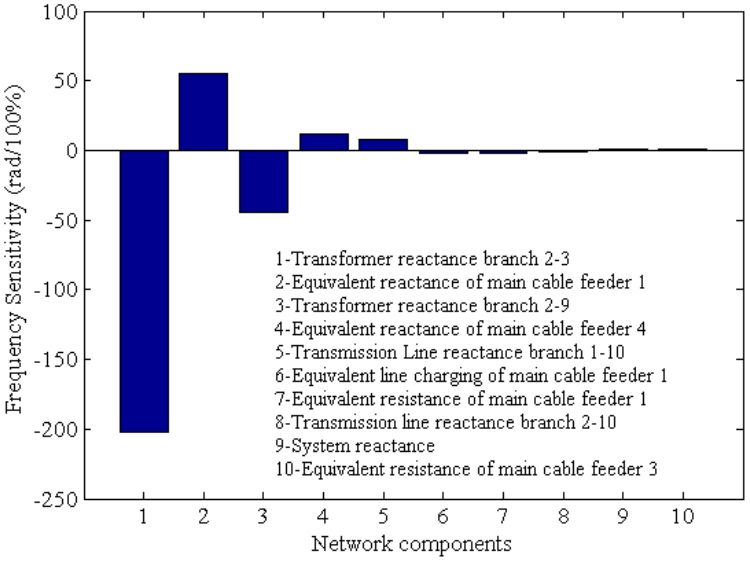

Figure 5.15 Frequency sensitivity at h = 45.8

As observed in Figure 5.6, magnitude of modal impedance is insignificant in comparison with other modal impedance at previous resonant frequencies. The modal impedance is used to predict the severity of the harmonic resonance; thus, the severity of the resonance between the 45th and 46th harmonics is not significant. This is also represented by sensitivity indices calculated in Tables 5.10 and 5.11.

- **At resonant frequency h = 47.5**

The eigen and frequency sensitivity indices are tabulated in Tables 5.12 - 5.13. Those graphs of these indices are shown in Figures 5.16 – 5.17 respectively.

Table 5.12 Eigen sensitivity at h = 47.5

No.	Components - α	$\frac{\partial \lambda}{\partial \alpha}(\%)$
1	Equivalent resistance of main cable feeder 3	447.685
2	Equivalent resistance of main cable feeder 5	397.163
3	Equivalent reactance of main cable feeder 3	377.98
4	Equivalent reactance of main cable feeder 5	299.427
5	Transmission Line reactance branch 1-10	3.7392
6	Equivalent line charging of main cable feeder 3	-1.8802
7	Equivalent reactance of pad-mount transformer feeder 5	-1.6768
8	Equivalent resistance of main cable feeder 1	1.1124
9	Transformer reactance branch 2-3	0.8809
10	Equivalent reactance of main cable feeder 2	0.8513

Table 5.13 Frequency sensitivity at h = 47.5

No.	Components - α	$\frac{\partial_f}{\partial \alpha}(\frac{rad}{100\%})$
1	Equivalent reactance of main cable feeder 3	-43.479
2	Equivalent reactance of main cable feeder 5	-35.433
3	Transformer reactance branch 2-9	4.3723
4	Transformer reactance branch 2-3	2.9441
5	Equivalent line charging of main cable feeder 5	1.117
6	Equivalent line charging of main cable feeder 3	1.1127
7	Equivalent resistance of main cable feeder 5	0.2479
8	Equivalent resistance of main cable feeder 3	0.2417
9	Equivalent reactance of main cable feeder 1	-0.1133
10	Equivalent reactance of main cable feeder 2	-0.1016

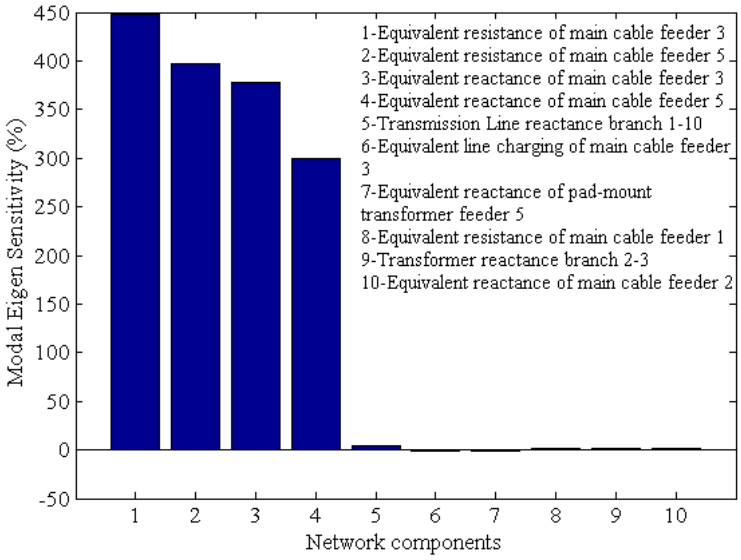

Figure 5.16 Eigen-sensitivity at h = 47.5

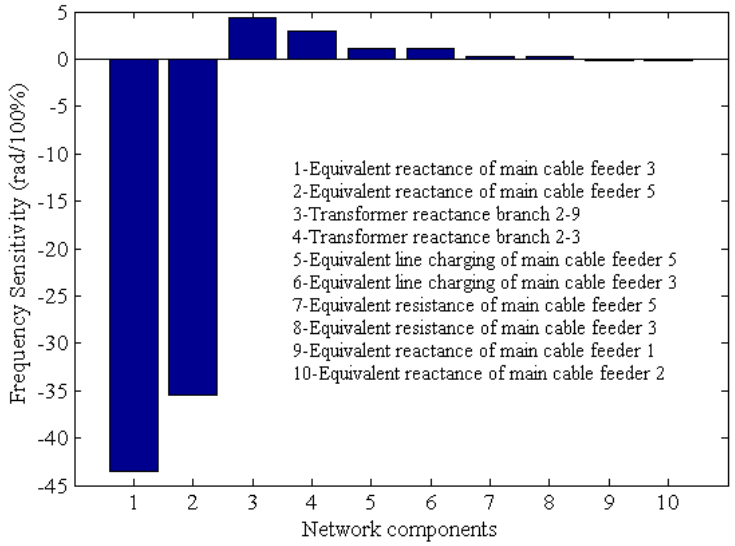

Figure 5.17 Frequency sensitivity at h = 47.5

As similar to the resonance between 45th and 46th harmonics, the resonance in this case is not severe. However, it seems that the influences of the wind power plant on harmonic resonance are more considerable than the previous cases when most of the largest sensitivity indices related to parameters of equivalent components of the wind power plant.

- **Resonance Paths**

From those sensitivity indices calculated above, resonance paths corresponding to each resonant frequency are plotted in Figure 5.18. The frequency sensitivity indices are mainly used to plot resonance paths because the influences of these indices on

harmonic resonance are more accurate than that with eigen-sensitivity indices. However, in case, frequency sensitivity indices are comparable, the eigen - sensitivity indices are used to identify which components are more sensitive to resonant frequency.

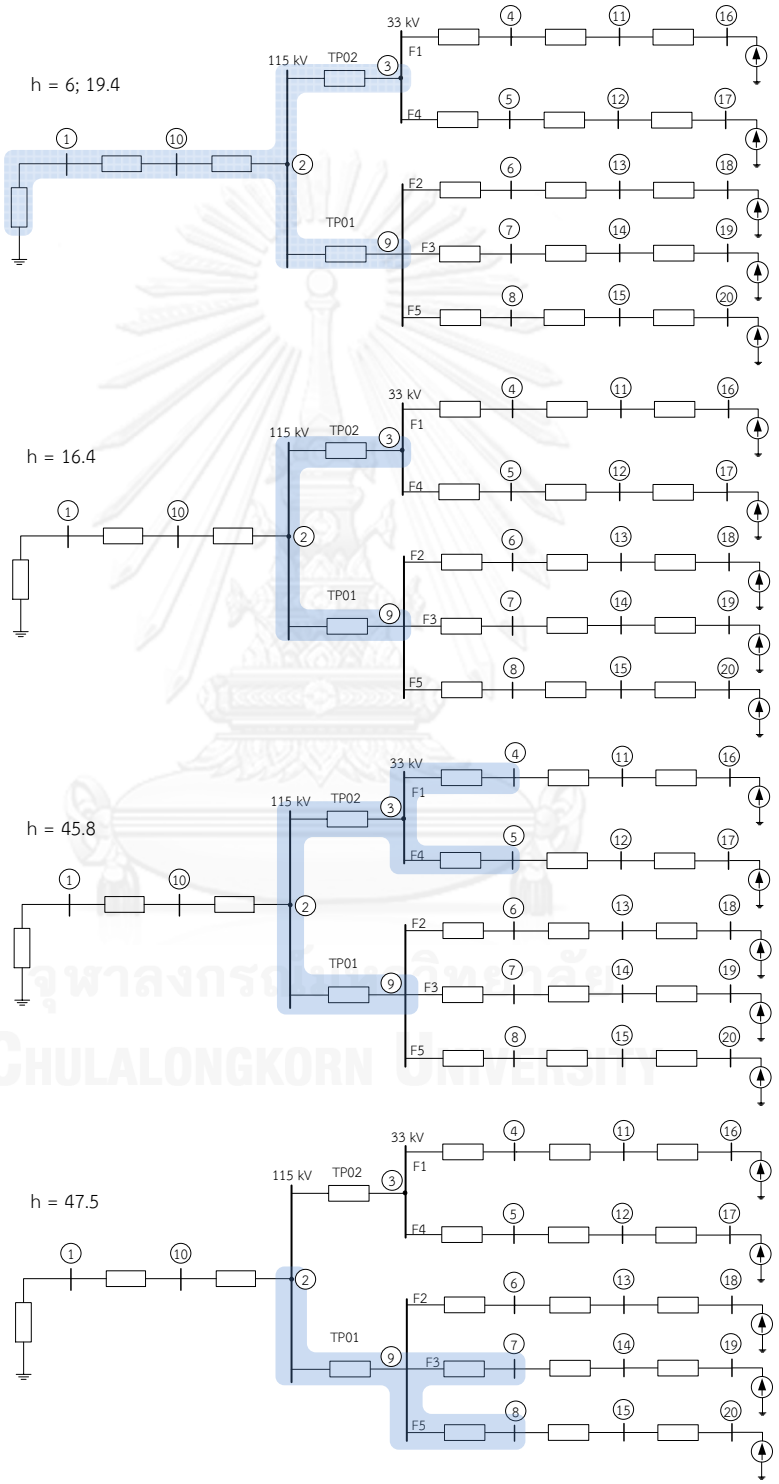

Figure 5.18 Resonance Paths

5.1.2.2 Scenario 2

The test system is balanced, and the wind turbine generators connected to different sections of 33 kV bus bar match balance power generation condition. As a result, only group 1, which is depicted in Figure 5.3, will be taken into account for calculation of sensitivity indices. The frequency scan based on harmonic resonance analysis is conducted. Figure 5.19 shows system responses corresponding to cases of only group 1 or 2 in operation, and Table 5.14 tabulates simulation results.

Table 5.14 Harmonic resonant frequencies in p.u

	HRMA	Frequency Scan Analysis	
		At 115 kV bus	At 33 kV bus
Only group 1 in operation	7; 18.5; 45.4	7; 18.5	7; 18.5; 45.4
Only group 2 in operation	6.8; 18.2; 47.4	6.8; 18.2	6.8; 18.2

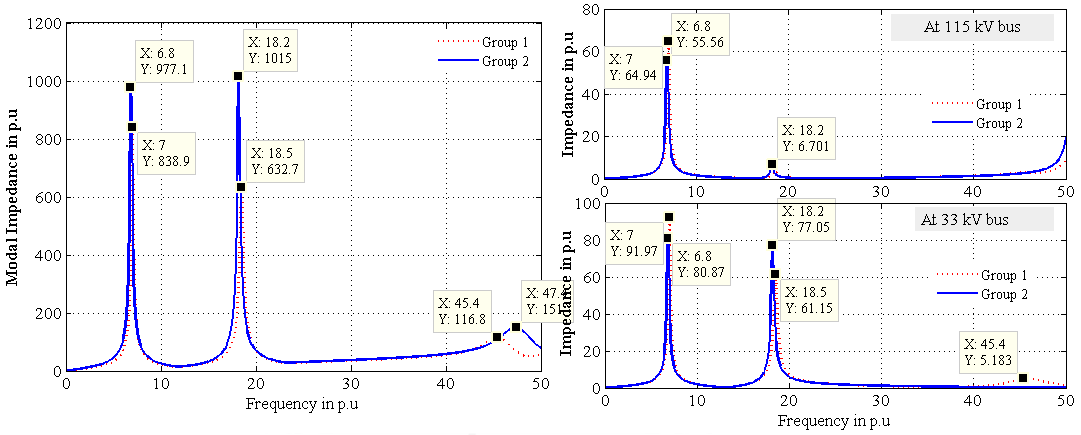

a. **Modal Frequency Scan Analysis** **b. Frequency scan analysis**

Figure 5.19 System responses

There is not a significant difference between simulation results by considering different groups of wind turbine generators in operation due to the balanced system. Resonant frequencies obtained by both harmonic resonance mode and frequency scan analyses are consistent. Harmonic resonance mode analysis can figure out entirely possible harmonic resonant frequencies in the system in a unique plot while frequency scan analysis requires scanning at every bus in system. Therefore, harmonic resonance analysis points out another harmonic resonance between 47th and 48th harmonics as shown in Figure 5.19.

The sensitivity calculation is conducted in case of the group 1 in operation. Since the system is balanced as explained previously, it is unnecessary to calculate sensitivity indices in both cases. Tables 5.15-5.20 show calculation results, and Figures 5.20 - 5.25 illustrate graphs of sensitivity indices at resonant frequencies respectively.

- At resonant frequency h = 7

Table 5.15 Eigen sensitivity at h = 7

No.	Components - α	$\frac{\partial \lambda}{\partial \alpha}$(%)
1	Transformer reactance branch 2-3	-2212.91
2	System resistance	-1332.44
3	System reactance	-584.299
4	Transmission line resistance branch 1-10	-105.911
5	Transmission line reactance branch 1-10	-43.3764
6	Transmission Line reactance branch 2-10	-29.9763
7	Transformer resistance branch 2-3	-10.1794
8	Equivalent resistance of main cable feeder 1	-2.1612
9	Transmission line resistance branch 2-10	1.5999
10	Equivalent resistance of main cable feeder 4	-0.3478

Table 5.16 Frequency sensitivity at h = 7

No.	Components - α	$\frac{\partial f}{\partial \alpha}(\frac{rad}{100\%})$
1	System resistance	-15.6984
2	Transformer reactance branch 2-3	10.6139
3	Transmission Line reactance branch 2-10	-3.0272
4	Transmission line resistance branch 1-10	-1.2448
5	System reactance	0.8216
6	Transformer resistance branch 2-3	-0.5565
7	Transmission line reactance branch 1-10	0.2962
8	Equivalent resistance of main cable feeder 1	-0.0269
9	Transmission line resistance branch 2-10	0.0134
10	Equivalent resistance of main cable feeder 4	-0.0044

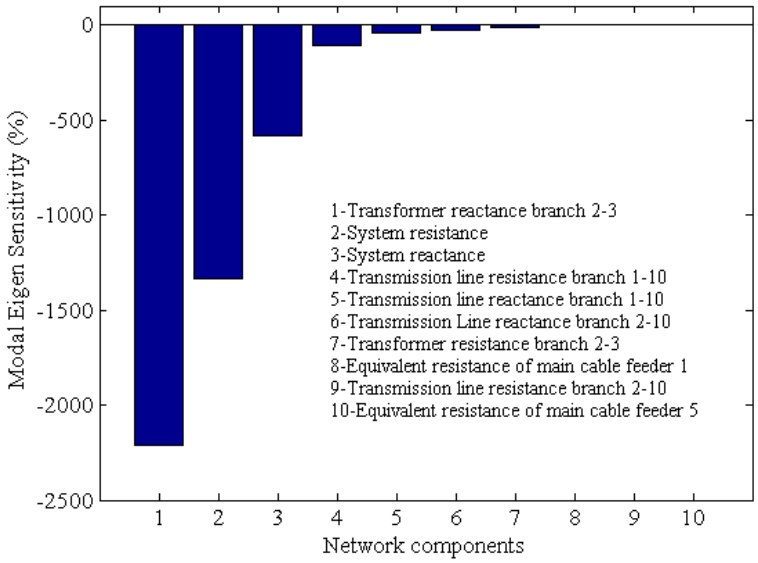

Figure 5.20 Eigen-sensitivity at h = 7

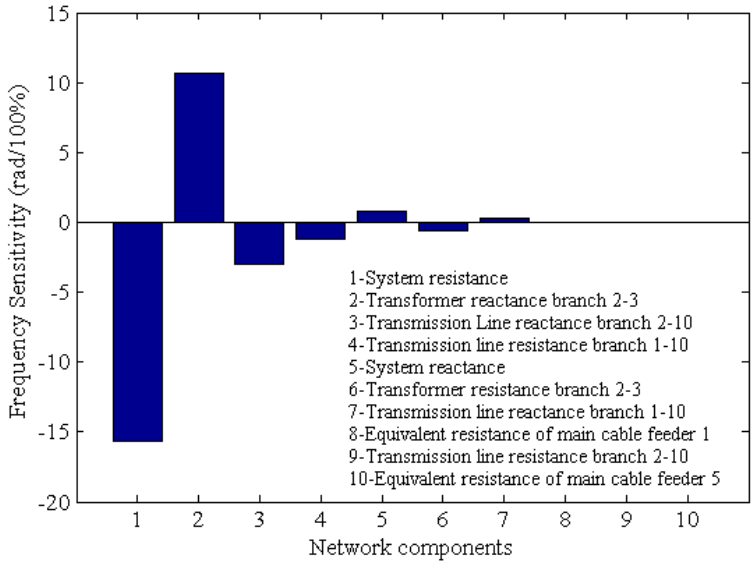

Figure 5.21 Frequency sensitivity at h = 7

Sensitivity indices show that the most participated network components in the harmonic resonance around the 7^{th} harmonic belong to main grid. The sensitivity with respect to changes of equivalent components of the wind farm is inconsiderable.

- At resonant frequency h = 18.5

Table 5.17 Eigen sensitivity at h = 18.5

No.	Components - α	$\frac{\partial \lambda}{\partial \alpha}$(%)
1	Transformer reactance branch 2-3	-50983.1
2	Transformer resistance branch 2-3	2807.578
3	System reactance	-895.075
4	System resistance	-517.75
5	Transmission Line reactance branch 2-10	-353.027
6	Transmission line reactance branch 1-10	-151.184
7	Equivalent resistance of main cable feeder 1	-123.795
8	Transmission line resistance branch 1-10	-87.0964
9	Equivalent reactance of main cable feeder 1	-25.9226
10	Transmission line resistance branch 2-10	22.3798

Table 5.18 Frequency sensitivity at h = 18.5

No.	Components - α	$\frac{\partial f}{\partial \alpha}(\frac{rad}{100\%})$
1	Transformer reactance branch 2-3	-2630.01
2	Transformer resistance branch 2-3	45.8339
3	Transmission Line reactance branch 2-10	-32.2901
4	System reactance	-8.1963
5	System resistance	-7.1474
6	Equivalent resistance of main cable feeder 1	-1.8812
7	Transmission line resistance branch 1-10	-1.236
8	Transmission line reactance branch 1-10	-1.1094
9	Equivalent reactance of main cable feeder 1	-0.3552
10	Transmission line resistance branch 2-10	0.3485

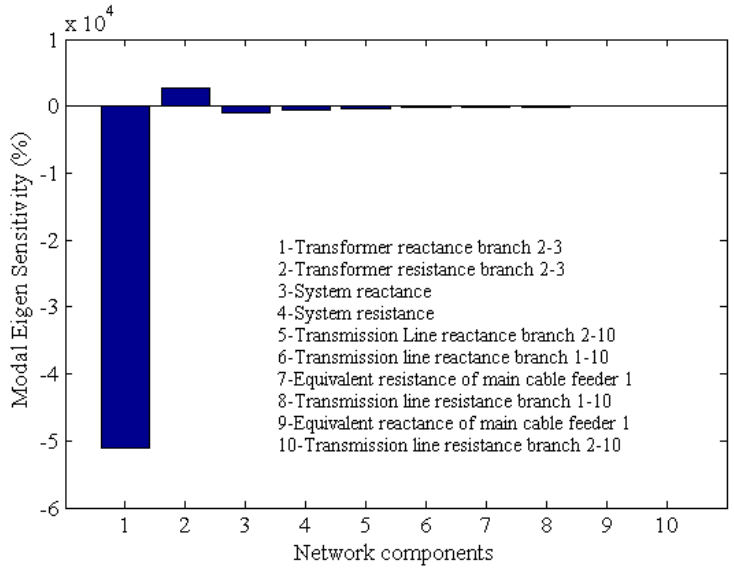

Figure 5.22 Eigen-sensitivity at h = 18.5

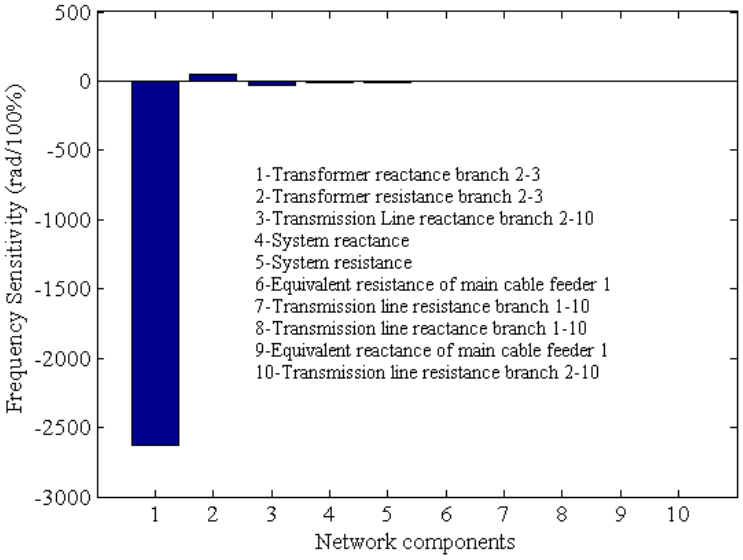

Figure 5.23 Frequency sensitivity at h = 18.5

Calculation of sensitivity indices in this case also point out similar observation to the resonance around the 7^{th} harmonic. The grid still affects mainly the harmonic resonance.

- At resonance frequency h = 45.4

Table 5.19 Eigen sensitivity at h = 45.4

No.	Components - α	$\frac{\partial \lambda}{\partial \alpha}(\%)$
1	Equivalent resistance of main cable feeder 1	-611.223
2	Equivalent reactance of main cable feeder 1	-451.961
3	Transmission line reactance branch 1-10	-443.853
4	Transformer reactance branch 2-3	-96.5799
5	Equivalent resistance of main cable feeder 4	-88.7523
6	System reactance	-84.0941
7	Equivalent resistance of main cable feeder 4	-51.1184
8	Equivalent reactance of pad-mount transformer feeder 1	34.9157
9	Equivalent reactance of pad-mount transformer feeder 4	29.2059
10	Transformer resistance branch 2-3	11.8928

Table 5.20 Frequency sensitivity at h = 45.4

No.	Components - α	$\frac{\partial f}{\partial \alpha}(\frac{rad}{100\%})$
1	Transformer resistance branch 2-3	-89.3632
2	Equivalent reactance of main cable feeder 1	-20.009
3	Transmission line reactance branch 1-10	-7.6396
4	Equivalent resistance of main cable feeder 1	-6.0295
5	Equivalent line charging of main cable feeder 1	2.4647
6	Transmission line reactance branch 2-10	-1.8437
7	System reactance	-1.8011
8	Equivalent resistance of main cable feeder 4	-0.6905
9	Equivalent reactance of main cable feeder 1	0.5639
10	Equivalent reactance of pad-mount transformer feeder 1	-0.3931

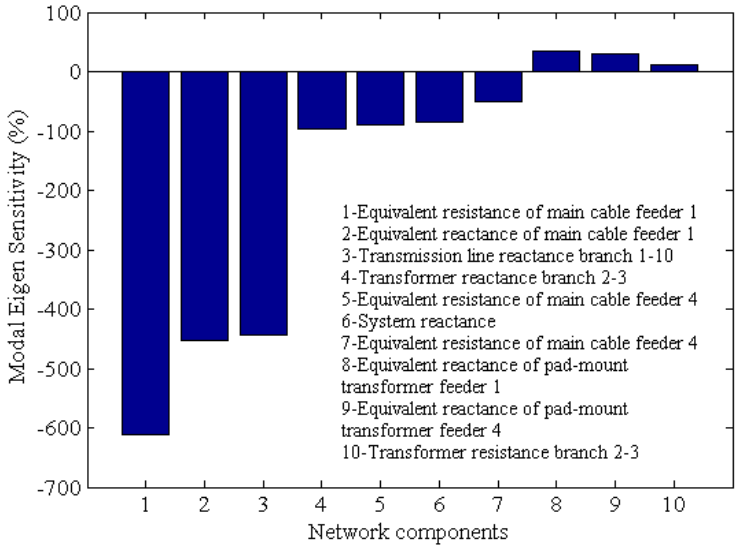

Figure 5.24 Eigen-sensitivity at h = 45.4

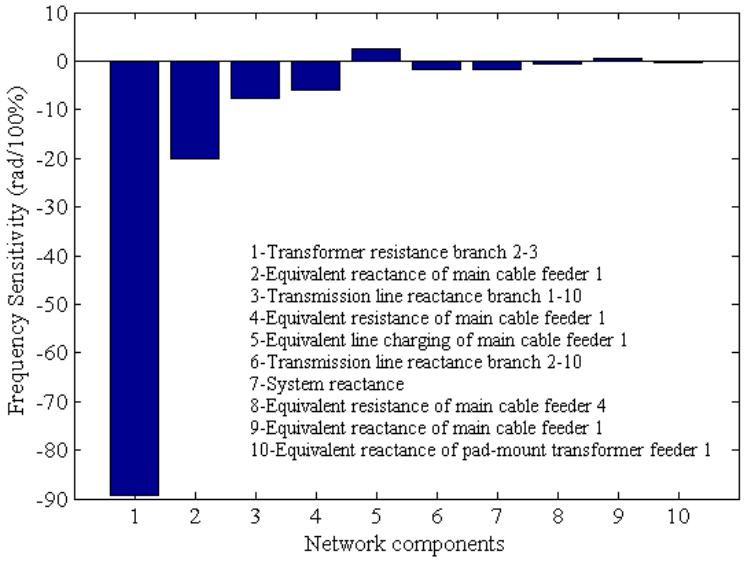

Figure 5.25 Frequency sensitivity at h = 45.4

In the area of high frequencies, the participation of the wind farm component in harmonic resonance becomes more significant. In other words, harmonic resonances in the area of high frequencies are likely to happen due to the wind farm. However, the most significant component to the resonance between the 45^{th} and 46^{th} harmonics is step up transformer. The wind farm can affect considerably severity of resonances because the largest eigen-sensitivity index is the sensitivity with respect to equivalent resistance of main feeder 1.

Based on the indices in Tables 5.15 - 5.20 and those graphs shown in Figure 5.20 - 5.25, resonance paths corresponding to resonant frequencies are plotted in Figure 5.26.

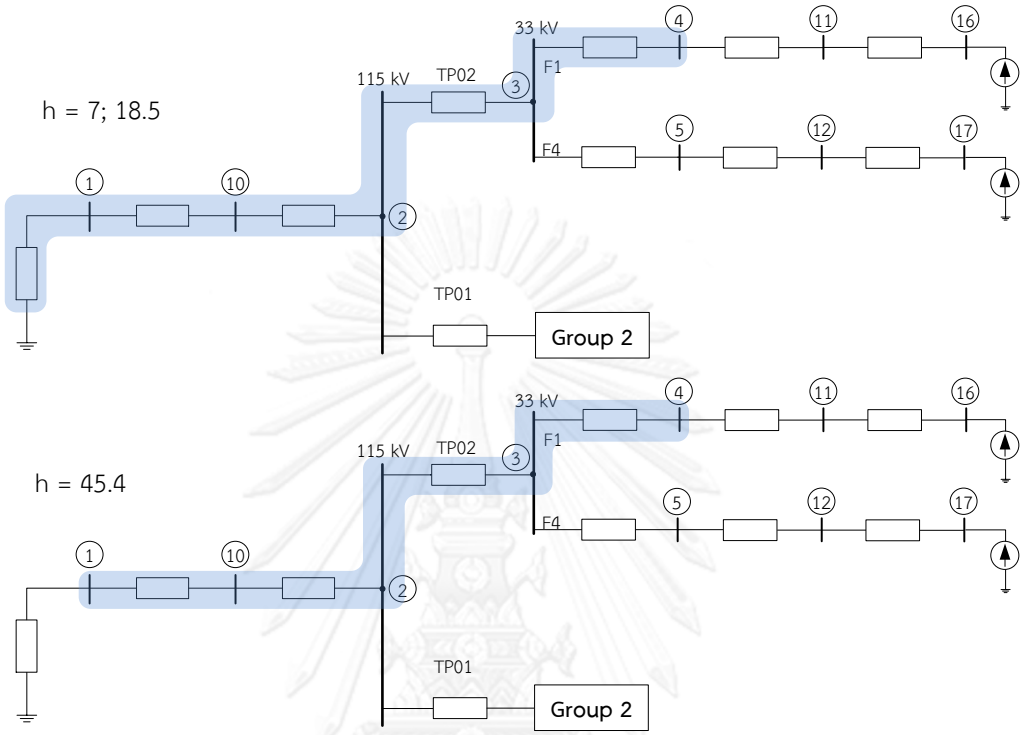

Figure 5.26 Resonance paths

All in all, from the simulation results, some noticeable conclusions are given as follows.

1. The most dominant harmonics found are close to 6th and 16th harmonics. The simulation results predict the resonances surrounding the 6th harmonic can be the severest problem.
2. Most participated components affecting significantly harmonic resonances in the systems connected with the wind power plant are system impedance, transmission line and transformers. The wind power plant also participates in harmonic resonances; however, this participation is not as appreciable as the network components in main grid are mentioned.
3. The order of most participated network components is changed with distinct resonant frequencies. At the area of low frequency, the resonance is likely to result from mainly step up transformers.
4. Harmonic resonant frequencies found when wind power plants are modeled as an EOCC or EOML are quite close to each other. However, the results

found using EOCC must be reasonable because EOCC model partially includes entire components of medium voltage systems. The simulation results found by using EOML bring a good prediction for harmonic resonances.

5. By considering two scenarios, frequency scan based on harmonic resonance mode analysis points out that resonant frequencies are shifted by various operation of the wind power plants. Particularly, resonant frequencies found in system with only group 1 of the wind power plant in operation tend to be shifted to the area of lower frequencies. It is because the influences of the cables in the wind power plant on harmonic resonances. Even though the sensitivity indices show that the main participated network components in harmonic resonances belong to main grid, the impacts of medium voltage networks on harmonic resonances at both high and medium voltage buses are unavoidable.
6. There is no harmonic resonance happening in the area of high frequency at 115 kV bus, but there are two resonances observed at 33 kV buses. The resonance paths show that there are more network components of wind power plants participating in when harmonic resonances happen in this area of frequency.

5.2 Verification with Actual Measurement Data

The procedure of verification has been explained in detail in chapter 4. The location of meters used in collecting data has been described in Figure 5.3 as well. Since the number of meters is limited, only the frequency scan results at 115 kV and 33 kV buses are taken into account for verifying with actual measurement data. In simulation, harmonic resonances have been pointed out by conducting harmonic resonance mode analysis. The resonant frequencies calculated by both modal and frequency scan analyses at both 115 kV and 33 kV buses are consistent. Therefore, the verification with resonant frequency found at these buses is completely reasonable to validate the results found by using harmonic resonance mode analysis. Table 5.21 and Figure 5.27 summarize those simulation results, and Figure 5.28 illustrates the configuration of test system with equipped meters. The frequency scan at those buses paid attention is also depicted in Figure 5.28.

Table 5.21 Resonant frequencies at 115 kV and 33 kV buses

	Resonant frequencies in p.u	
Bus	Scenario 1	Scenario 2
115 kV bus (bus 2)	6 ; 19.4	6.8 ; 18.2 ;
33 kV bus (bus 3)	6 ; 16.4 ; 19.4 ; 45.4	6.8 ; 18.2 ; 45.4

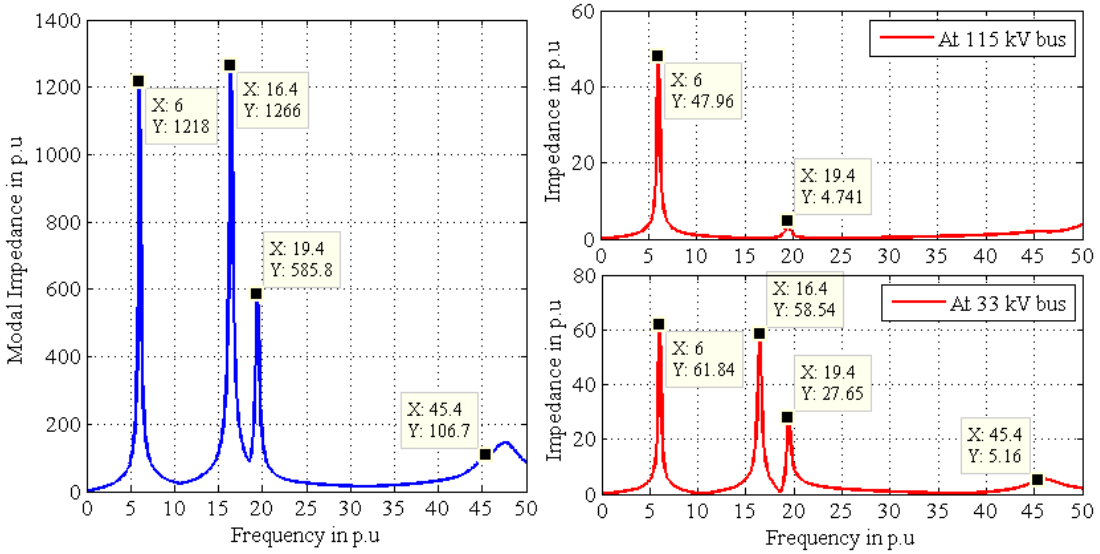

a. Harmonics resonance mode analysis b. Frequency scan analysis

Figure 5.27 System response at 115 kV and 33 kV buses with full wind turbines in operation

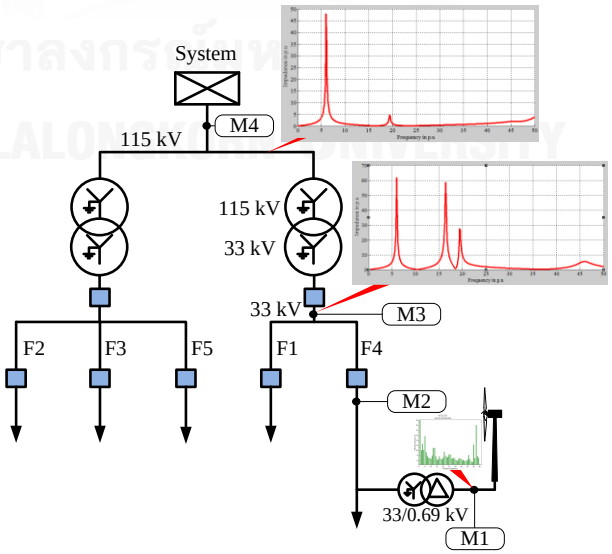

Figure 5.28 The test system configuration with equipped meters

Harmonic resonances lead to very high harmonic voltage distortion. This index is used as an indicator to identify harmonic resonances from actual measurement data. The total voltage distortion at 115 kV and 33 kV buses is depicted in Figures 5.29 and 5.30 respectively.

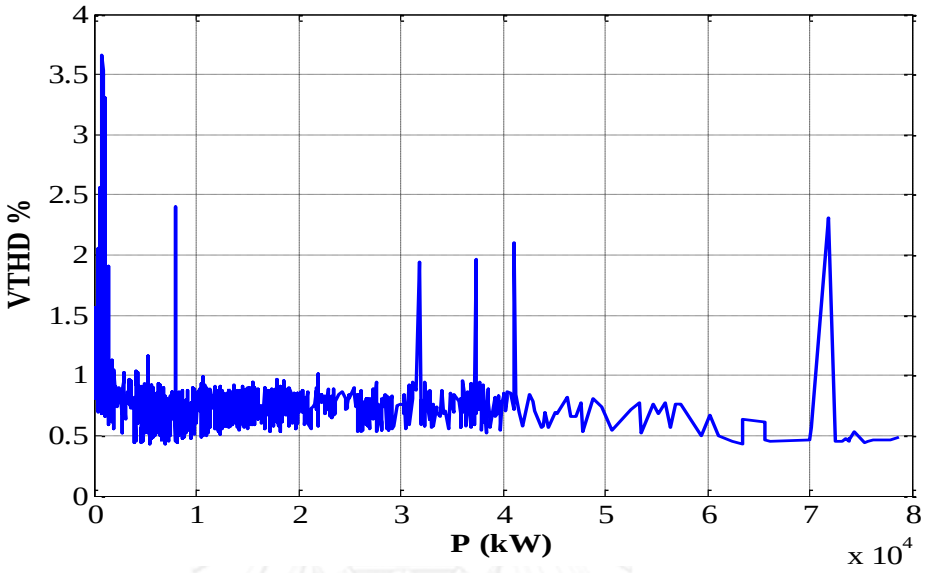

Figure 5.29 Variation of harmonic distortion with respect to active power at 115 kV bus by meter M4

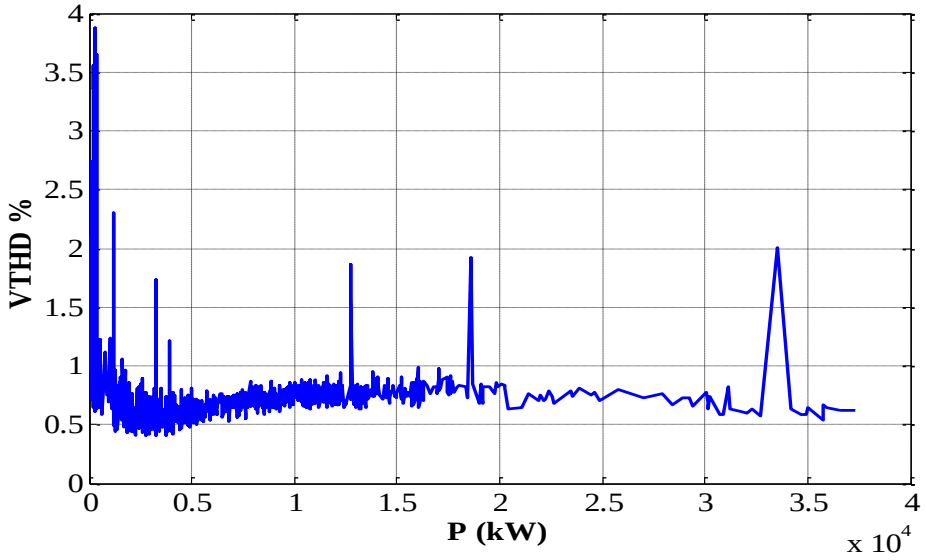

Figure 5.30 Variation of harmonic distortion with respect to active power at 33 kV bus by meter M2 and M3

The frequency scan analysis at 115 kV and 33 kV buses shows that two common resonant frequencies at these buses are observed at 6 and 19.4 harmonics. As

discussed in simulation results, harmonic resonances tend to shift to the area of low frequency. Thus, it is reasonable to state that harmonic resonances can happen at the frequency between 5th and 6th harmonics when the harmonic resonant order found is at 6, and the other resonance will happen at the frequency between 19th and 20th harmonics. At 33 kV buses, there are two other harmonic resonant frequencies observed, which are between 16th and 17th harmonics and between 45th and 46th harmonics.

As shown in Figures 5.29 and 5.30, some areas of high total voltage distortion are quite similar at both 115 kV and 33 kV buses. It might be explained by those common resonant frequencies between 5th and 6th and 19th and 20th harmonics. However, as illustrated in Figure 5.27, the magnitude of impedance seen at 115 kV bus at the frequency between 19th and 20th harmonics is not appreciable. It means that the harmonic resonance is unlikely to happen at this frequency.

5.2.1 Verification of Resonances at 115 kV Bus

At 115 kV bus, the actual measurement data recorded during 5th – 13th in March 2013 show that the 5th harmonic voltage coincides with the variation of total voltage distortion. The peaks of the 5th harmonic voltage considerably match up with peaks of total voltage distortion curve shown in Figure 5.31. In other words, the harmonic resonance is possible to happen at the 5th harmonic. Nonetheless, look at the data at the 6th harmonic voltage and total voltage distortion, the remaining peaks, which are not matched up with the 5th harmonic voltage, catch peaks of the 6th harmonic voltages. Figure 5.32 illustrates the variation of total harmonic voltage distortion and the 6th harmonic voltage.

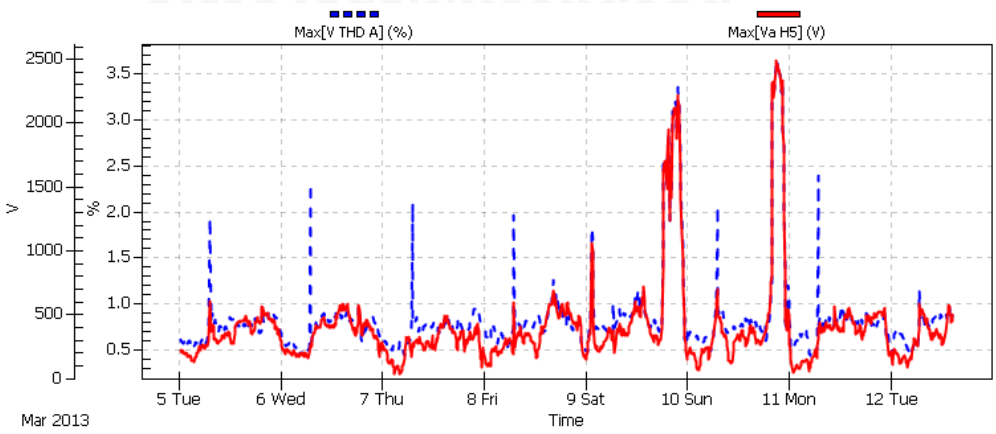

Figure 5.31 The 5th harmonic voltage and total harmonic voltage distortion

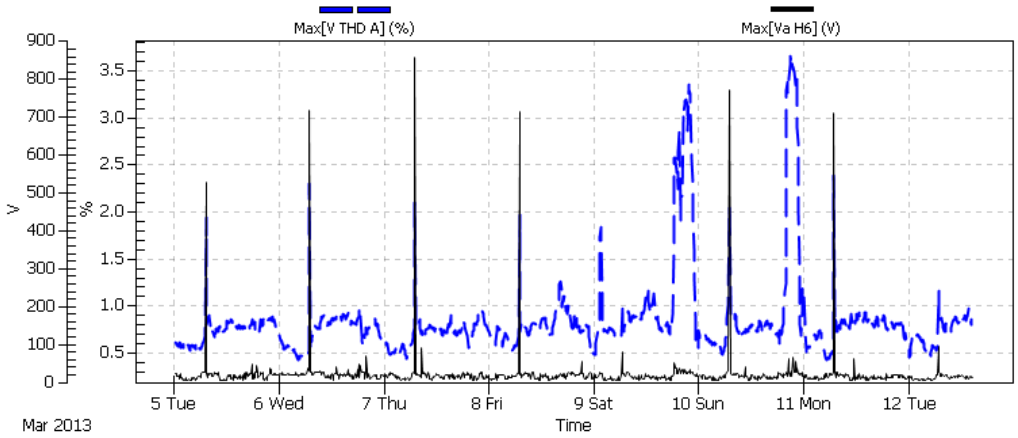

Figure 5.32 The 6th harmonic voltage and total harmonic voltage distortion

By analyzing the harmonic voltage spectrum at 115 kV bus as shown in Figure 5.33, actual measurement data show that harmonic resonances are possible to happen at both 5th and 6th harmonics. However, the 5th harmonic is still the most dominant component in harmonic spectrum, and the influence of the amplification of the 5th harmonic is severer than that of the 6th harmonic. Particularly as illustrated in Figure 5.33, the amplification of the 5th harmonic is three times as large as the 6th harmonic is amplified in resonances. Moreover, the fact that high harmonic voltage distortion resulting from the amplification of the 5th harmonic take place longer than that is observed with the 6th harmonic. The short duration of the 6th harmonic amplification is not a significant sense of resonances. In other words, the severity of the harmonic resonance at the 6th is not a big problem to the system, which can be seen more clearly in analyzing the voltage at 115 kV in time domain as shown in Figure 5.34.

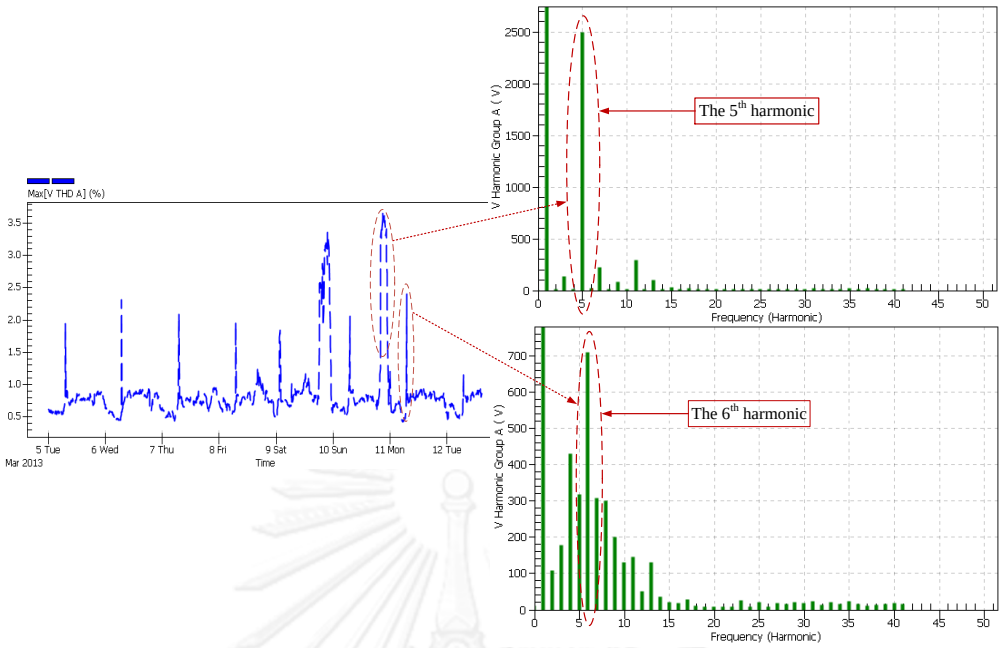

Figure 5.33 The harmonic voltage spectrum at 115 kV bus

Corresponding to the harmonic spectrum in Figure 5.33, Figure 5.34 shows the different influences of resonances at 5th and 6th harmonics on waveforms of voltage at 115 kV bus. While the amplification the 5th harmonic results in considerable distortion of the waveform, the waveform seem to be unaffected by the 6th harmonic amplified.

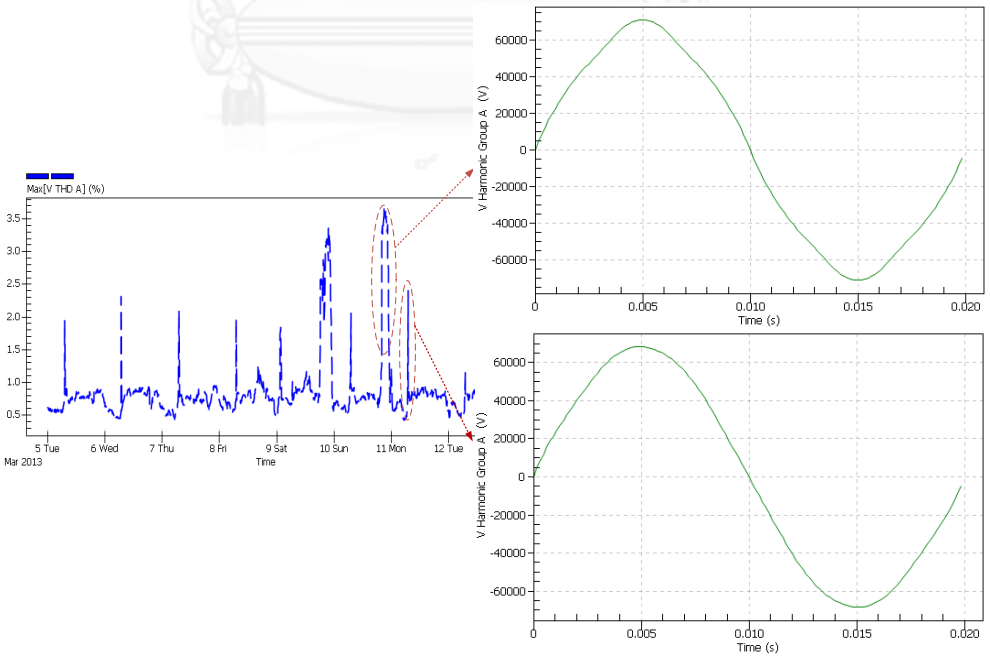

Figure 5.34 The voltage waveforms at 115 kV bus corresponding to the 5th and 6th harmonics amplified

By doing similar procedure previously, there is no harmonic resonance observed at the 7th harmonic at both 115 kV and 33 kV buses. The resonance in simulation at frequency between 19th and 20th harmonics is not considerable; moreover, actual measurement data do not show any correlation that it is possible for harmonic resonances at this frequency. Figure 5.35 illustrates 19th and 20th harmonic voltages.

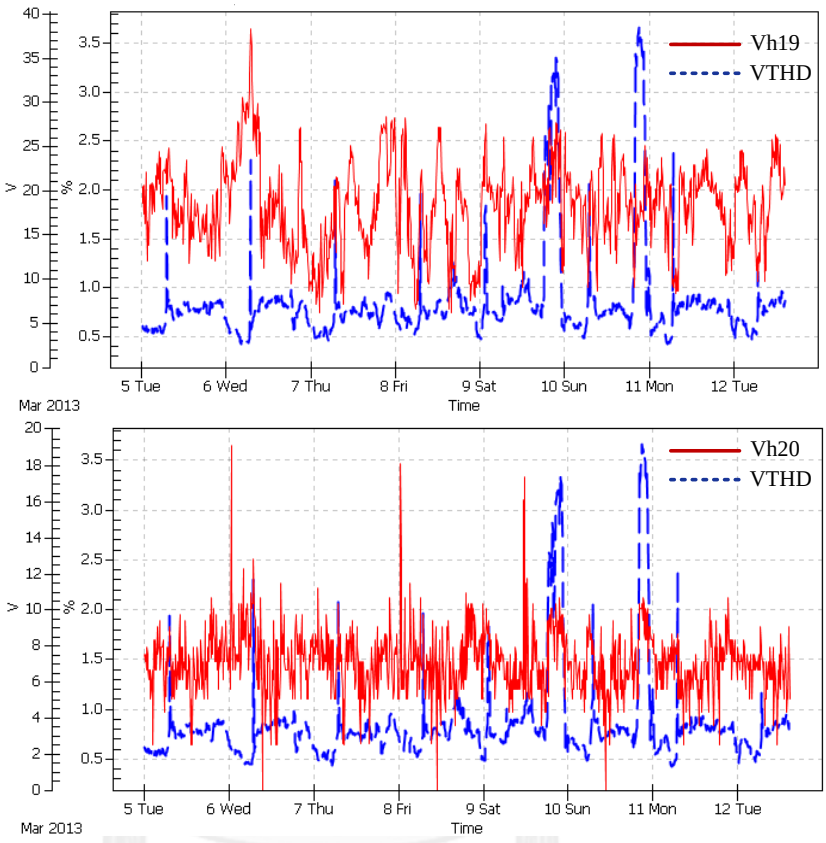

Figure 5.35 The 19th and 20th harmonic voltages

5.2.2 Verification of Resonances at 33 kV Bus

By analogy with the verification of the 5th harmonic resonance at 115 kV bus, actual measurement data also point out that the harmonic resonance also happens at the 5th harmonic. The actual measurement data show similar observation as considered at 115 kV bus. However, the harmonic resonance recorded only happens at the 5th harmonic. The 5th harmonic is dominant components, and its amplification is more appreciable than the others.

Figures 5.36 – 5.39 illustrate the observation from actual data recorded during 5th – 13th in March 2013.

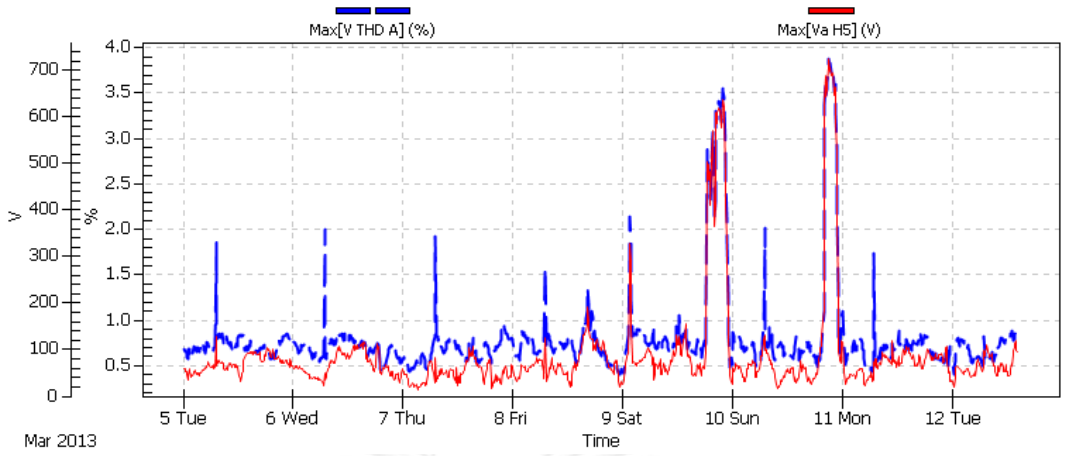

Figure 5.36 The 5th harmonic voltage and total harmonic voltage distortion

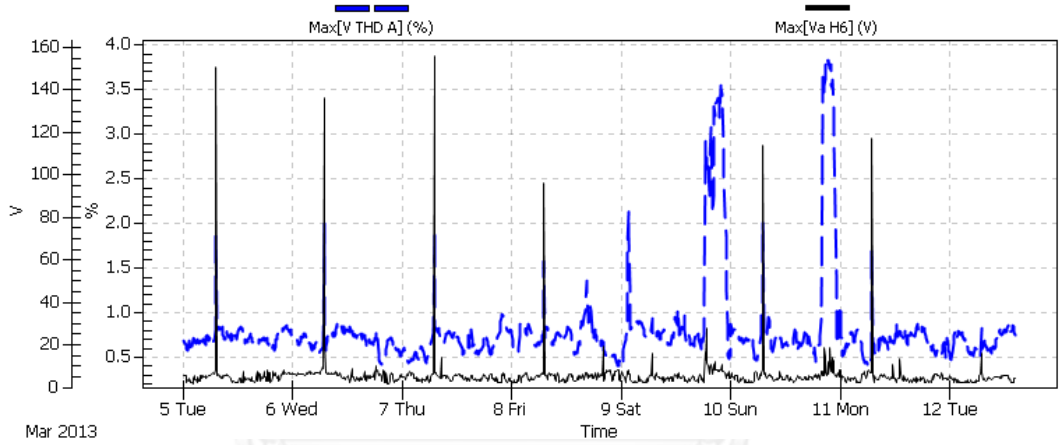

Figure 5.37 The 6th harmonic voltage and total harmonic voltage distortion

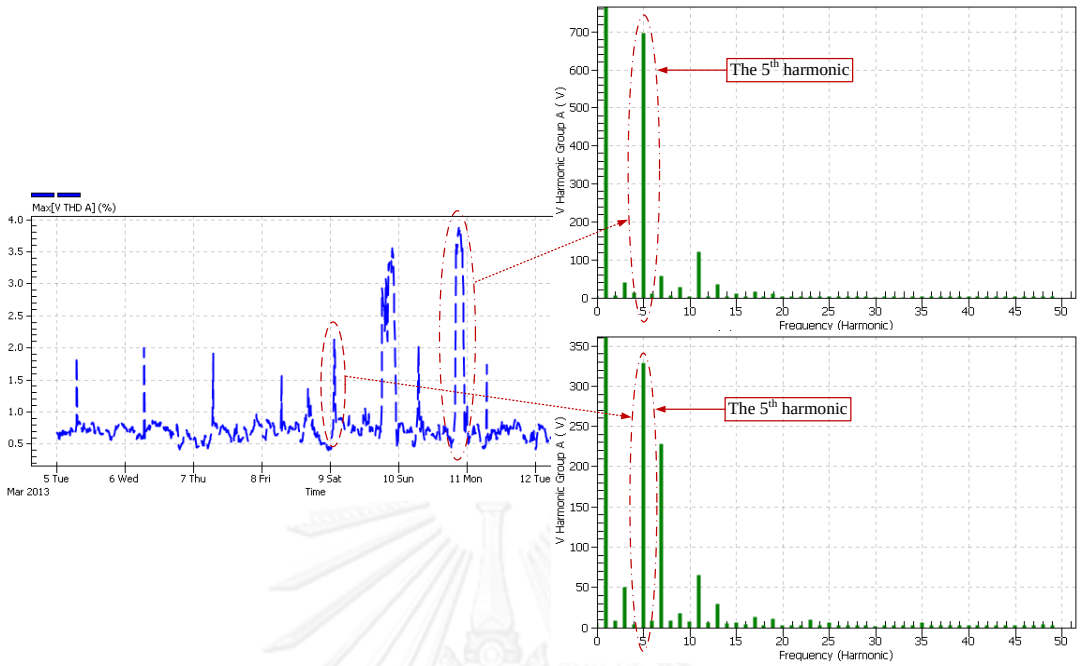

Figure 5.38 The harmonic voltage spectrum at 33 kV bus

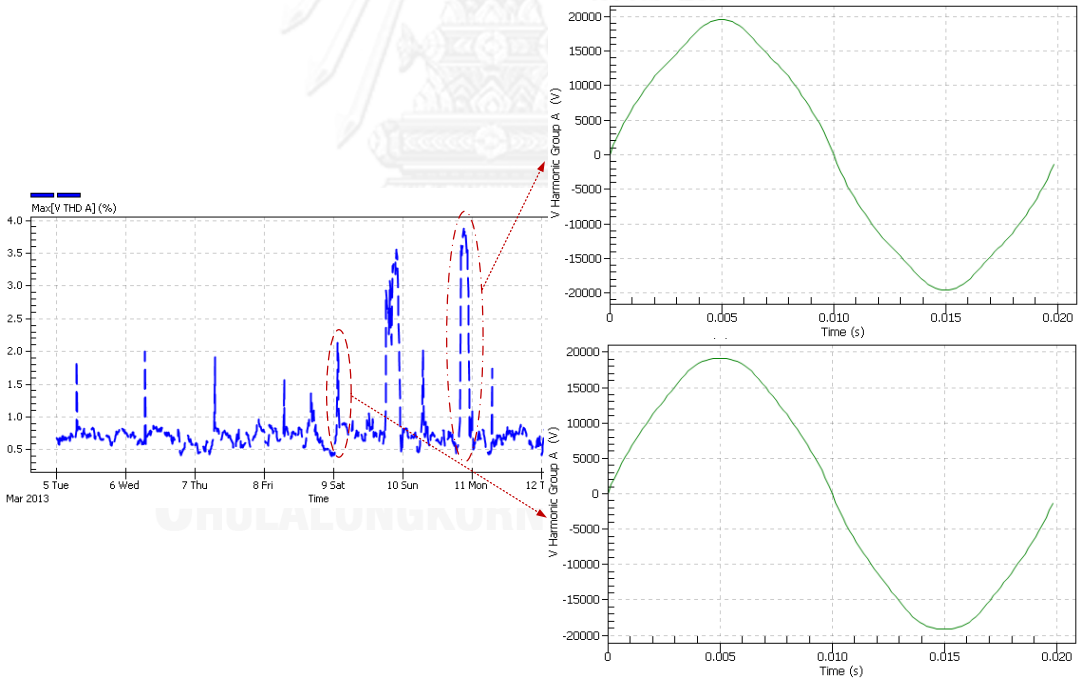

Figure 5.39 The voltage waveforms at 33 kV bus

To verify harmonic resonance at the frequency between 16th and 17th harmonics and between 19th and 20th harmonics, the voltages at these harmonics are shown in Figure 5.40.

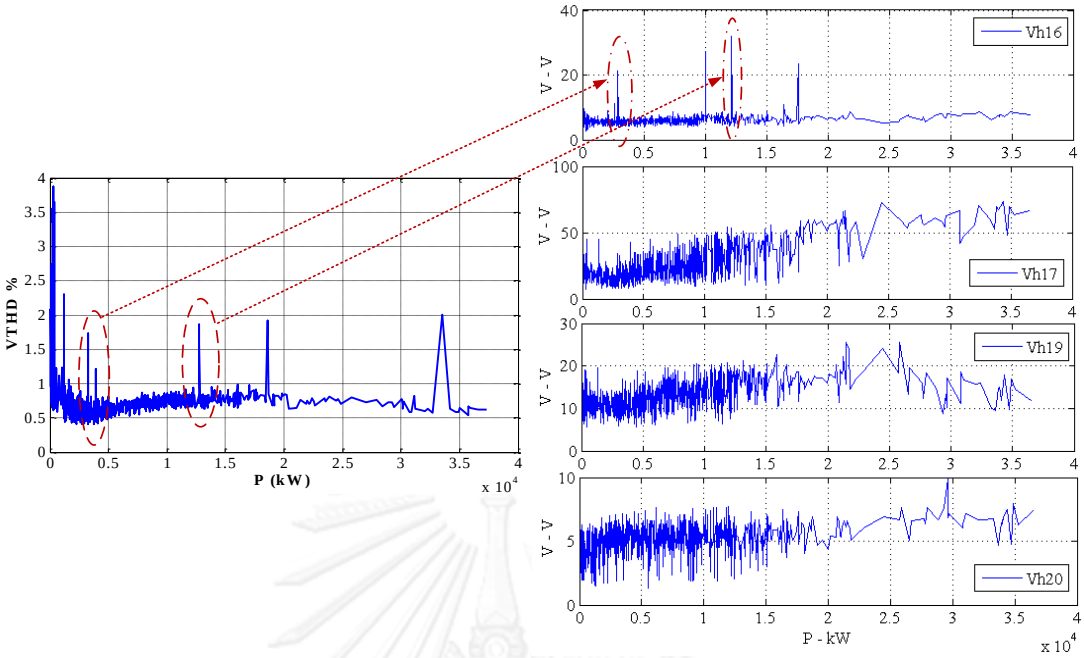

Figure 5.40 Harmonic voltages

As observed in Figure 5.40, the harmonic voltage is amplified at the 16th and the peaks observed match with the peaks of total harmonic distortion curve shown in the figure as well. There is no corresponding point observed at the other harmonic frequencies. Therefore, it can be stated that the simulation also points out the resonance at the 16th harmonic, but resonance does not happen between 19th and 20th harmonics.

The last frequency need to be verified is between 45th and 46th harmonics. These harmonic voltages are plotted with respect to active power as in Figure 5.41.

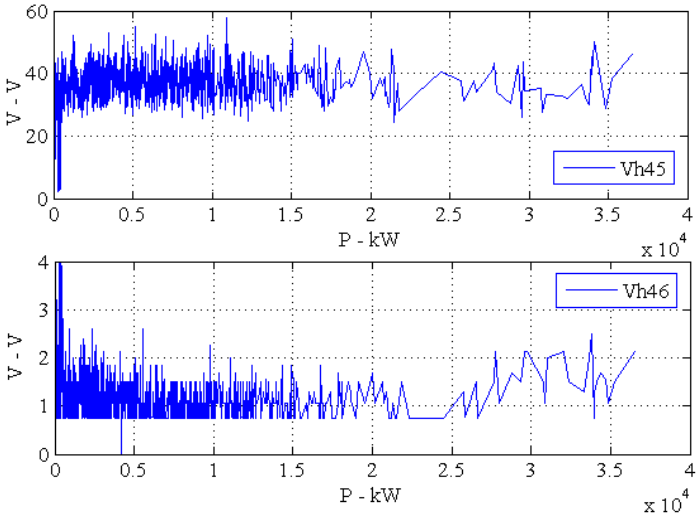

Figure 5.41 Harmonic voltages

As illustrated in Figure 5.41, harmonic resonance does not happen at the frequency between 45th and 46th harmonics. It is likely to match with the frequency scan analysis, which shows that the magnitude of impedance seen at 33 kV bus at 45.4 is not significant, and the field measurement data clarify this prediction.

5.3 Discussion

The two scenarios drawn in the study shows the shifts of harmonic resonances in various operation modes of the wind power plant. The particular influence of the operation of wind power plants represented in shifts of resonant frequencies in area of low frequency.

The verification show that the simulation results match considerably with the field measurement. Identification of harmonic resonances in area of low frequencies is quite accurate. However, there is a deviation from harmonic resonances in area of high frequencies; simulation results do not match with field measurement. It might be explained because the wind power plant does not generate an appreciable content of harmonics in this area of frequencies. Figure 5.42 depicts harmonic generation at the recorded time when total harmonic distortion reaches the highest point at both 115 kV and 33 kV buses. The most dominant harmonic is the 5th, so the harmonic resonance resulting from the 5th is observed most clearly in verification.

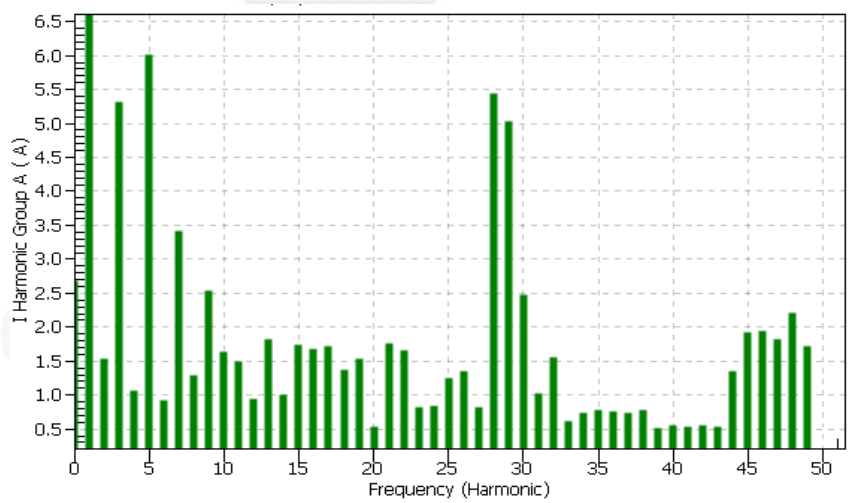

Figure 5.42 Harmonic generation of a wind turbine generator at the highest harmonic voltage distortion at 115 kV and 33 kV buses

The 6th harmonic also results in amplification of voltage at both 115 kV and 33 kV buses, which the peaks of the harmonic voltage curve match quite well with the peaks of total harmonic distortion curve. However, the sudden amplification of the 6th harmonic voltage at both observed buses is not big problem because the

content of the 6^{th} harmonic is not significant. The similar observation also comes along with the 16^{th} harmonic. The harmonic resonance is possible at the 16^{th} harmonic at 33 kV when some peaks of the 6^{th} voltage curve match with the corresponding peaks of total harmonic distortion curve.

The results verified show that harmonic resonance mode analysis is a useful tool for harmonic resonance analysis though the deviation exists between simulation results and field measurement data. The deviation can be explained due to some resonance including the harmonic models used in simulation, and specially the model of the wind power plant

CHAPTER VI

Conclusion and Future Work

6.1 Conclusion

Harmonic resonance mode analysis has been conducted in a practical system with a wind power plant connected in order to figure out the harmonic resonance problems. Potential harmonic resonances, which have been verified with field measurement, confirm the validity of this method. Some conclusions of the study are summarized as follows.

1. Harmonic resonance mode analysis potentially points out all possible harmonic resonances existing in the electric power system. Instead of running frequency scan analysis at all buses as traditional procedure of frequency scan analysis, frequency scan based on harmonic resonance mode analysis is taken into account as a time saving technique in simulation. In verification with field measurement at 115 kV and 33 kV buses, the simulation results found by using this method cover entirely resonant frequencies found by using frequency scan analysis.
2. The severity of resonances is revealed in simulation with harmonic resonance mode analysis. The field measurement data has partially validated this issue.
3. The information provided by harmonic resonance mode analysis including participation factors and sensitivity indices is useful to construct harmonic resonance paths, which reveal main components affecting harmonic resonances. The field measurement data have not verified elaborately this point in verification.
4. The deviation between simulation results and field measurement data still exists. The differences can be understandable when considering those issues:
    - The limitation of the model of wind power plants can affect simulation results. The aggregate model supports time saving simulation and provides good prediction for harmonic resonances; nonetheless, the requirement of absolute accuracy is still a difficult task. In other words, the simulation results can only cover a large range of possible resonant frequencies, which can contain some of actual potential resonant frequencies.

- The limitation of harmonic models of network components can also influence on simulation results.

6.2 Future Work

Harmonic resonance analysis in power systems with wind power plants has done at some points. Furthermore, the study needs more investigations in the following issues.

1. Assessing the severity of possible harmonic resonances has not been worked out well. This information will be significantly imperative in harmonic resonance assessment. As a result, this task should be paid more attention.
2. The verification with actual measurement data needs more data in order to verify the simulation results more accurately, especially the validation of sensitivity indices.
3. The simulation results indicate that impacts of the system configuration on harmonic resonances is more momentous than that of wind power plants' operation condition. This is because the harmonic generation of wind power plants has not documented well in the harmonic model. A deeper investigation into harmonic emission needs to be done in order to assess completely the influences of harmonic resonances on network components.
4. Harmonic resonance mode analysis is just applied for balanced system. Conducting this method in three phase system is necessary to provide whole picture about the applicability of the method.

REFERENCES

1. IEEE - 519 Standard: IEEE Recommended Practices and Requirements for Harmonic Control in Electrical Power Systems. 1992.
2. IEC Standards Part 3 - 6: Limits - Assessment of Emission Limits for The Connection of Distoring Installation to MV, HV And EHV Power System. 2008.
3. R. C. Dugan, M. F. McGranaghan, S. Santoso, and H.Wayne Beaty, Electrical Power Systems Quality. 2 ed. 2012: McGraw-Hill.
4. J. Li, N. Samaan, and S. Williams. Modeling of Large Wind Farm Systems for Dynamic and Harmonics Analysis. in IEEE PES Transmission Distribution Conference. 2008.
5. Z. Chen, J. M.Gurrero, and F. Blaabjerg, A Review of The State of The Art of Power Electronics for Wind Turbines. IEEE Transaction on Power Electronics, 2009. **24**(8): p. 17.
6. B. Wu, Y. Lang, N. Zargari, and S. Kouro, Power Conversion and Control of Wind Energy Systems, I. Press, Editor. 2011, John Wiley and Sons.
7. T. Ackermann, Wind Power in Power Systems. 2 ed. 2012: John Wiley and Sons.
8. O. Anaya-Lara, N. Jenkins, J. Ekanayake, P. Cartwright, M. Hughes, Wind Energy Generation Modeling and Control. 2009: John Wiley and Sons.
9. IEC Standard 61400 - 21: Wind Turbine Generator Systems – Part 21: Measurement and Asessment of Power Quality Characteristics of Grid Connected Wind Turbines. 2008.
10. Z. Huang, Y. Cui, and W. Xu, Application of Modal Sensitivity for Power System Harmonic Resonance Analysis. IEEE Transaction on Power Delivery, 2007. **22**(1): p. 10.
11. S. L. Varricchio, N. Martins, and R. De Janeiro, Filter Design Using A Newton-Raphson Method Based On Eigenvalue Sensitivity, in IEEE Power Energy Society General Meeting. 2000.
12. S. Gomes Jr, N. Martins, C. Portela, Modal Analysis Applied to s-Domain Models of AC Networks. in IEEE Power Engineering Society Winter Meeting. 2001.
13. S. L. Varricchio, N. Martins, and L. T. G. Lima, A Newton-Raphson Method Based on Eigenvalue Sensitivities to Improve Harmonic Voltage Performance, in IEEE Power Energy Society General Meeting. 2003.
14. S. Varricchio, S. J. Gomes, and N. Martins, Modal Analysis of Industrial System Harmonics Using The S - Domain Approach, in IEEE Power Energy Society General Meeting. 2004.
15. W. Xu, Z. Huang, Y. Cui, and H. Wang, Harmonic Resonance Mode Analysis. IEEE Transaction on Power Delivery, 2005. **20**(2): p. 9.

16. J. Arrillaga and N. Watson, Power System Harmonics. 2 ed. 2004: John Wiley and Sons.
17. W. Xu and J. García-mayordomo, Three - Phase Power Flow and Harmonic Analysis. Electric Energy Systems Analysis and Operation. 2009.
18. Y. Cui and W. Xu, Assessment of Potential Harmonic Problems for Systems with Distributed or Random Harmonic Sources, in IEEE Power Energy Society General Meeting. 2007.
19. Y. Cui and W. Xu, Harmonic Resonance Mode Analysis Using Real Symmetrical Nodal Matrices. IEEE Transaction on Power Delivery., 2007. **22**(3): p. 2.
20. M. Esmaili, H. Ali Shayanfar, and A. Jalilian, Modal analysis of power systems to mitigate harmonic resonance considering load models. Elsevier Journal of Energy, 2008. **33**(9): p. 8.
21. C. Amornvipas and L. Hofmann, Resonance Analyses in Transmission Systems: Experience in Germany, in IEEE Power Energy Society General Meeting. 2010.
22. Y. Cui and X. Wang, Modal Frequency Senstivity for Power System Harmonic Resonance Analysis. IEEE Transaction on Power Delivery., 2012. **27**(2): p. 8.
23. R. Bellman, Introduction to Matrix Analysis. 1960: John Wiley and Sons.
24. S. Gomes Jr, N. Martin, C Portela, s - Domain Approach to Reduce Harmonic Voltage Distortion Using Sensitivity Analysis, in IEEE Power Engineering Society Winter Meeting. 2001.
25. S. L. Varricchio, Sergio Gomes. Jr, N. Martins, L. R. Araujo, F. C. Véliz, and C. De O. Costa, IX Symposium of Specialists in Electric Advanced Tool for Harmonic Analysis of Power System. 2004.
26. E. Muljadi, S. Pasupulati, A. Ellis, and D. Kosterov, Method of Equivalencing for A Large Wind Power Plant with Multiple Turbine Representation, in IEEE Power Energy Society General Meeting. 2008.
27. F. Ghassemi and K. Koo, Equivalent Network for Wind Farm Harmonic Assessments. IEEE Transaction on Power Delivery, 2010. **25**(3): p. 8.
28. R. Zheng, M. H. J. Bollen, and J. Zhong, Harmonic Resonances due to A Grid-Connected Wind Farm, in The 14th International Conference on Harmonics and Quality of Power. 2010.
29. K. Yang and M. Bollen, Theoretical Emission Study of Windpark Grids, in The 11th International Conference on Electrical Power Quality and Utilisation (EPQU). 2011.

30. B. Badrzadeh, M. Gupta, N. Singh, A. Petersson , and M. Høgdahl, Power System Harmonic Analysis in Wind Power Plants - Part I : Study Methodology and Techniques, in IEEE Industry Application Society Annual Meeting (IAS). 2012.
31. G. A. Mendonça, H. A. Pereira, and S. R. Silva, Wind Farm and System Modelling Evaluation in Harmonic Propagation Studies, in International Conference on Renewable Energies and Power Quality (ICREPQ). 2012.
32. S. A. Papathanassiou and M. P. Papadopoulos, Harmonic Analysis in a Power System with Wind Generation. IEEE Transaction on Power Delivery, 2006. **21**(4): p. 11.
33. R. King, and J. Ekanayake, Harmonic Modelling of Offshore Wind Farms, in IEEE Power Energy Society General Meetig. 2010.
34. E. Muljadi, C. P. Butterfield, A. Ellis, J. Mechenbier, J. Hochheimer, R. Young, N. Miller, R. Delmerico, R. Zavadil, and J. C. Smith, Equivalencing The Collector System of A Large Wind Power Plant, in IEEE Power Energy Society General Meetig. 2006.
35. J. Brochu, C. Larose, and R. Gagnon, Validation of Single- and Multiple-Machine Equivalents for Modeling Wind Power Plants. IEEE Transaction of Energy Conversion, 2011. **26**(2): p. 10.
36. J. Brochu, C. Larose, and R. Gagnon, Generic Equivalent Collector System Parameters for LargeWind Power Plants. IEEE Transaction of Energy Conversion, 2011. **26**(2): p. 8.
37. C. Larose, R. Gagnon, P. Prud'Homme, M. Fecteau, and M. Asmine, Type-III Wind Power Plant Harmonic Emissions: Field Measurements and Aggregation Guidelines for Adequate Representation of Harmonics. IEEE Transaction of Sustainable Energy, 2013: p. 8.
38. H. Chu Xuan and T. Tayjasanant, Modeling Wind Power Plants in Harmonic Resonance Study - A Case Study in Thailand. in The 5th International Conference on Information Technology and Electrical Engineering (ICITEE). 2013.
39. T. Tayjasanant, Lecture Note - Fundamentals of Power Quality. 2012.
40. W. Xu, Component Modeling Issues for Power Quality Assessment. IEEE Power Energy Review, 2001. **21**(11): p. 6.
41. A. Bonner, T. Grebe, E. Gunther, L. Hopkins, M. B. Marz, J. Mahseredjian, T. H. Omneyer, V. Rajagopalan, S. J. Ranade, P. FXbeiro, T. R. Sims, and W. Xu, Modeling and Simulation of The Propagation in Electric Power Networks - Part I: Concepts, Models, and Simulation Techniques. IEEE Transaction on Power Delivery, 1996. **11**(1): p. 14.
42. W. Wiechowski and P. Eriksen, Selected Studies on Offshore Wind Farm Cable Connections-Challenges and Experience of the Danish TSO, in IEEE Power Energy

Society General Meeting - Conversion and Delivery of Electrical Energy in the 21st Century. 2008.

APPENDIX

Network and the wind power plant data

Network Data

Table A. 1. Network impedance in P.U based on 100 MVA

	R	X	B	Section
System	0.02706	0.1736	0	-
Transmission	0.0192	0.1198	0.03377	1
Line	0.0019	0.0119	0.00338	2
Transformer 115/33 kV	0.0033	0.1333	0	-

Wind Power Plant Data

Table A.2 Impedances of cables of main feeders 1, 2, 3, and 4 in P.U based on 100 MVA

	R	X	B	No.WTGs
Feeder 1	0.011	0.008	0.0024	5
	0.0117	0.0132	0.0012	1
	0.0104	0.0117	0.0011	1
	0.006	0.0067	0.0006	1
	0.008	0.009	0.0008	2
	0.053	0.0598	0.0055	1
Feeder 2	0.0072	0.0066	0.0005	3
	0.0105	0.0119	0.0011	2
	0.028	0.0316	0.0029	2
Feeder 3	0.0355	0.0325	0.0026	3
	0.0074	0.0084	0.0008	4
	0.0525	0.0593	0.0054	2
Feeder 4	0.0118	0.0071	0.0004	2
	0.0095	0.0087	0.0007	1
	0.0133	0.015	0.0014	1
	0.0189	0.0213	0.0019	2
	0.02	0.0226	0.0021	2
	0.0139	0.0157	0.0014	3

Table A.3 Impedances of cables of the main feeder 5 in P.U based on 100 MVA

	R	X	B	No.WTGs
Feeder 5	0.0096	0.0087	0.0007	3
	0.0064	0.0072	0.0007	1
	0.0046	0.0052	0.0005	1
	0.0164	0.0185	0.0017	1
	0.0517	0.0583	0.0053	1

* The impedance of each section along each feeder is listed from the furthest section to the collector bus. No.WTGs stands for number of wind turbine generators.

Table A.4 Impedances of cables connecting between main feeders 1, 4 and pad-mount transformers in P.U based on 100 MVA

To feeder 1			To feeder 4		
R	X	B	R	X	B
0.00261	0.00067	2.55E-05	0.00261	0.00067	2.55E-05
0.03129	0.00804	0.002359	0.00261	0.00067	2.55E-05
0.00261	0.00067	2.55E-05	0.00261	0.00067	2.55E-05
0.00261	0.00067	2.55E-05	0.00261	0.00067	2.55E-05
0.00261	0.00067	2.55E-05	0.02973	0.00764	0.000291
0.0217	0.00558	0.000212	0.00261	0.00067	2.55E-05
0.00261	0.00067	2.55E-05	0.04355	0.01119	0.000426
0.00261	0.00067	2.55E-05	0.00261	0.00067	2.55E-05
0.00261	0.00067	2.55E-05	0.03437	0.00884	0.000336
0.00261	0.00067	2.55E-05	0.00261	0.00067	2.55E-05
0.0471	0.01211	0.00046	0.02206	0.00567	0.000216

Table A.5 Impedances of cables connecting between main feeders 2, 3 and pad-mount transformers in P.U based on 100 MVA

To feeder 2			To feeder 3		
R	X	B	R	X	B
0.03568	0.00917	0.000349	0.00261	0.00067	2.55E-05
0.00261	0.00067	2.55E-05	0.01773	0.00456	0.000173
0.05044	0.01296	0.000493	0.04454	0.01145	0.000435
0.06238	0.01603	0.00061	0.04235	0.01089	0.000414
0.00261	0.00067	2.55E-05	0.00261	0.00067	2.55E-05
0.00261	0.00067	2.55E-05	0.04861	0.0125	0.000475
0.00261	0.00067	2.55E-05	0.05737	0.01475	0.000561
-	-	-	0.04506	0.01158	0.00044
-	-	-	0.00261	0.00067	2.55E-05

Table A.6 Impedances of cables connecting between the main feeders 5 and pad-mount transformers in P.U based on 100 MVA

To feeder 5		
R	X	B
0.05216	0.01341	0.00051
0.01857	0.00477	0.000181
0.00261	0.00067	2.55E-05
0.00261	0.00067	2.55E-05
0.00261	0.00067	2.55E-05
0.00261	0.00067	2.55E-05
0.00595	0.00153	5.81E-05

Table A.7 Impedances of pad – mount transformers in P.U based on 100 MVA corresponding to feeders 1 and 4

To feeder 1		To feeder 4	
R	X	R	X
0.255556	2.003333	0.255556	2.02
0.255556	1.966667	0.255556	2.096667
0.255556	1.986667	0.255556	2.066667
0.255556	1.993333	0.255556	2
0.255556	1.953333	0.255556	2.156667
0.255556	1.923333	0.255556	1.986667
0.255556	2.116667	0.255556	1.976667
0.255556	2.07	0.255556	1.953333
0.255556	2.143333	0.255556	2.13
0.255556	2.153333	0.255556	2.066667
0.255556	2.026667	0.255556	1.966667

Table A.8 Impedances of pad – mount transformers in P.U based on 100 MVA corresponding to feeders 2 and 3

To feeder 2		To feeder 3	
R	X	R	X
0.255556	2.173333	0.255556	2.023333
0.255556	2.16	0.255556	2.15
0.255556	2.063333	0.255556	2.113333
0.255556	2.156667	0.255556	1.996667
0.255556	2.153333	0.255556	1.996667
0.255556	2.056667	0.255556	2.003333
0.255556	2.036667	0.255556	1.983333
-	-	0.255556	0.255556
-	-	0.255556	1.966667

Table A.9 Impedances of pad – mount transformers in P.U based on 100 MVA corresponding to feeder 5

To feeder 5	
R	X
0.255556	1.953333
0.255556	1.94
0.255556	1.986667
0.255556	1.96
0.255556	2.003333
0.255556	2.046667
0.255556	2.156667

* Note: each row of the table corresponds to parameters of a pad – mount transformer used to connect to the main feeder.

Table A.10 Impedances of asynchronous generators in p.u based on 100 MVA

R	X
0.294	0.895

VITA

Mr. Chu Xuan Huan was born in Bac Giang, Vietnam in 1988. He received the Bachelor's Degree of Electrical Engineering from Hanoi University of Science and Technology in 2011. He has been granted a scholarship by AUN/Seed-Net (JICA) to pursue the Master's Degree at Chulalongkorn University, Thailand since 2011. He conducted his research with Power System Research Laboratory at Department of Electrical Engineering, Faculty of Engineering His research interests include power quality, wind power plant modeling and renewable energy.